Pergamon

Geochimica et Cosmochimica Acta, Vol. 61, No. 1, pp. 219–237, 1997

0016-7037/97 $17.00 + .00

PII S0016-7037(96)00336-5

Carbide-magnetite assemblages in type-3 ordinary chondrites

ALEXANDER N. KROT,[1,2,*] MICHAEL E. ZOLENSKY,[3] JOHN T. WASSON,[1] EDWARD R. D. SCOTT,[2] KLAUS KEIL,[2] and KAZUMASA OHSUMI[4]

[1]Institute of Geophysics and Planetary Physics, University of California Los Angeles, Los Angeles, California 90095, USA
[2]Hawaii Institute of Geophysics and Planetology, School of Ocean and Earth Science and Technology, University of Hawaii at Manoa, Honolulu, Hawaii 96822, USA
[3]Earth Science and Solar System Exploration Division, NASA, Johnson Space Center, Houston, Texas 77058, USA
[4]Photon Factory, National Institute of High Energy Physics, Tsukuba, Japan

(*Received March* 7, 1996; *accepted in revised form September* 18, 1996)

Abstract—Abundant carbide-magnetite assemblages occur in matrix, chondrules, and chondrule rims in several H3, L3, and LL3 chondrites. Carbides, cohenite ($(Fe,Ni)_3C$), and haxonite ($(Fe,Ni)_{23}C_6$) show compositional variations between different meteorites and appreciable ranges within meteorites. Carbides in H chondrites have lower Co contents (0–0.6 wt%) than those in L and LL chondrites (0.3–1.2 wt%). Metal associated with carbides and magnetite consists of high-Ni (50–70 wt%) taenite and, in L and LL chondrites, Co-rich (up to 35 wt%) kamacite; minor element contents of troilite and magnetite are very low. Textural observations indicate that carbide-magnetite assemblages formed by replacement of metal-sulfide nodules. The high Co contents of residual kamacite in association with carbides indicates that Co is not incorporated into carbides (i.e., Fe/Co is much higher in the carbides than in kamacite). Because Ni in carbides and magnetite is low, the Ni contents of residual taenite tend to be high. Ni-rich sulfides were found only in LL3 chondrites, possibly indicating their more extensive oxidation and/or aqueous alteration.

We suggest that carbide-magnetite assemblages in type-3 ordinary chondrites formed as the result of hydrothermal alteration of metallic Fe in metal-troilite nodules by a C-O-H-bearing fluid on their parent bodies. This alteration resulted in carbidization of Fe-Ni metal, probably by CO gas (e.g., $15\ Fe(s) + 4\ CO(g) = Fe_3C(s) + Fe_3O_4(s)$ or $3\ Fe(s) + 2\ CO(g) = Fe_3C(s) + CO_2(g)$), and oxidation, probably by H_2O gas (e.g., $3Fe(s) + 4H_2O(g) = Fe_3O_4(s) + 4H_2(g)$). The C-O-H-bearing fluids, which were possibly released during metamorphism and transported through zones of high permeability, may have been derived from ices, adsorbed gases, or hydrated minerals. The CO may be the result of the reaction of carbon compounds (e.g., hydrocarbons) with water vapor or magnetite. *Copyright © 1997 Elsevier Science Ltd*

1. INTRODUCTION

An association consisting of magnetite, cohenite, $(Fe,Ni)_3C$, haxonite, $(Fe,Ni)_{23}C_6$, kamacite, troilite, and accessory taenite and pentlandite was originally described in LL3.0 Semarkona, LL3.7 ALHA77278, and LL3.2/3.7 Ngawi (Taylor et al., 1981). The nebular formation scenario for this assemblage proposed by Taylor et al. (1981) includes: reaction of metal with S at 700 K resulting in formation of troilite, carbidization of metal-troilite assemblages (reaction with graphite or gaseous CO or CH_4 to form cohenite and haxonite) at <450 K, accretion of matrix material, oxidation of metal-troilite-carbide assemblages at about 400 K and formation of magnetite, and additional accretion of magnetite. Hutchison et al. (1987) described carbide veins in Semarkona matrix and a carbide that might be intermediate between cohenite and ϵ-carbide (Fe_2C). They concluded that Semarkona experienced multistage nebular and parent body alteration, including possible formation of carbide-magnetite-metal assemblages due to gas-solid reaction between Fe-Ni metal and solar nebular gas (according to Taylor et al., 1981), accretion to a parent body, brecciation, magnetite and carbide crystallization, hydrous alteration, calcite precipitation, resorption of some magnetite, and maghemite precipitation. Fredriksson et al. (1989) studied magnetite-metal-troilite-cohenite-graphite nodules in the Study Butte H chondrite regolith breccia and suggested that these assemblages formed before agglomeration into the final parent body. Scott et al. (1982) identified haxonite in association with kamacite and taenite in LL3 ALHA79003, L3.6 Khohar, and LL3.4 Piancaldoli but did not discuss its origin.

Several iron carbides, including cohenite, ϵ-carbide, and an orthorombic Fe, Ni carbide, in association with Fe-Ni metal, magnetite, and iron sulfide were described in carbon-rich, chondritic interplanetary dust particles (IDPs) (Fraundorf, 1981; Christofferson and Buseck, 1983; Bradley et al., 1984). There is no consensus on the origin of carbides in IDPs; they were suggested to form by (a) heating and solid-solid reactions between metal grains and carbonaceous matrix material, (b) gas-solid reaction between metal and a carbidizing gas (CO?) produced internally on atmospheric entry, or (c) gas-solid reactions in the solar nebula during Fischer-Tropsch processes (Christofferson and Buseck, 1983; Bradley et al., 1984).

In this paper, we describe associations of Fe-Ni metal,

* Author to whom correspondence should be addressed (sasha@kahana.pgd.hawaii.edu).

troilite, carbides, and magnetite in a number of type-3 H, L, and LL chondrites. Based on textural observations and mineralogy, we conclude that carbide-magnetite assemblages formed by replacement of the metallic Fe metal-sulfide nodules. These unusual mineral assemblages, found only in ~10% of all type-3 ordinary chondrites (OCs), may offer important insights into the alteration processes and compositions of the fluids that operated in the solar nebula or in asteroids. Our final goal is to understand time, place, and relationship between various alteration processes, including aqueous alteration, alkali metasomatism, oxidation, and carbidization, which affected major components of ordinary and carbonaceous chondrites (chondrules, matrix materials, and Ca-, Al-rich inclusions).

2. ANALYTICAL PROCEDURES

More than 150 thin sections of 117 type-3 ordinary chondrites were studied in reflected and transmitted light using a Zeiss Universal petrographic microscope to search for carbides and magnetite (Table 1); twenty-five thin sections (Table 1) containing carbides and magnetite were studied in detail using electron-probe microanalysis (EPMA) and backscattered electron (BSE) imaging. Mineral phases were quantitatively analyzed with the UCLA Cameca Camebax electron probe using crystal spectrometers, counting times of 20 s, ZAF corrections, and a beam current of 15 nA at 15 kV. For metal and carbides the standards were pure Fe for Fe, NBS steel 1156 for Co (7.3 wt%) and Ni (19 wt%), NBS steel 483 for Si (3.2 wt%), chromite for Cr, and troilite from the Canyon Diablo iron meteorite for S; C was not analyzed. For silicates and magnetite the standards were grossular for Si, Ca, and Al, forsterite for Mg, magnetite for Fe, chromite for Cr, sphene for Ti, and spessartite for Mn.

We also prepared a few matrix samples of EET90161 for more detailed characterization by transmission electron microscopy (TEM). This was done using ultramicrotomed sections of grains embedded in EMBED-812 low-viscosity epoxy. We observed the microtomed sections at Johnson Space Center using a JEOL 2000FX STEM equipped with a LINK EDX analysis system. We used natural mineral standards and in-house determined k-factors for reduction of compositional data; a Cliff-Lorimer thin-film correction procedure was employed (Goldstein, 1979). Phyllosilicates were identified on the basis of both composition and electron diffraction data.

Although based on optical properties and/or Ni contents (for small carbide grains and veins), we divided carbides only into cohenite (anisotropic, <2 wt% Ni) and haxonite (isotropic, >4 wt% Ni), it seems possible that other carbide phases (e.g., $(Fe,Ni)_{2+x}C$) are also present (Scorzelli et al., 1996). Additional study using X-ray diffraction and Mössbauer spectroscopy is necessary to clarify this question. The identity of one high Ni carbide grain (haxonite) in Semarkona was verified using polychromatic synchrotron radiation with the Laue method at beamline 4B of the Photon Factory, National Institute of High Energy Physics, Tsukuba. In this experiment, a micro-pinhole collimator was used to constrain the incident X-ray beam to a diameter of 2.5 μm. An imaging plate (IP; Fuji Co., Ltd.) consisting of a two-dimensional detector coated with storage phosphors was used for data collection. The carbide grain was located in a standard petrographic thin section during the analysis. The techniques are described by Ohsumi et al. (1994).

Although high Ni contents in metal probably indicate the presence of tetrataenite (or even awaruite), our chemical and optical observations did allow tetrataenite and taenite to be resolved, and we call this metal Ni-rich taenite.

3. MINERALOGY AND CHEMISTRY OF CARBIDE-MAGNETITE ASSEMBLAGES

Carbide-magnetite assemblages (CMAs) were found in several H3, L3, and LL3 chondrites (Table 1). Based on the petrographic observations, as well as mineralogy and chemistry of CMAs, several Antarctic meteorites were reclassified and paired (see Table 2 and Appendix A). Although for the Antarctic type-3 OCs we use the petrographic subtypes listed by Grossman (1994), one should realize that this classification is preliminary.

Table 1. List of CMA-bearing type-3 ordinary chondrites.

chondrite	type	weath	sect	source	pairing
ALHA77278	LL3.7	A	43	MWG	
ALHA77278	LL3.7	A	98	MWG	
EET87735	L3.4	B	2	MWG	
EET90161	L3.4	B	2	MWG	E87735
EET90161	L3.4	B	4	MWG	E87735
EET90261	L3.4	Be	4	MWG	E87735
EET90519	L3.6	B/Ce	3	MWG	E87735
EET90628	L3.5	A/Be	4	MWG	E87735
Khohar	L3.6	fall	2363-1	SI	
LEW85434	L3.4	C	4	MWG	L86102
LEW85437	L3.4	C	4	MWG	L86102
LEW86102	H3.3	C	4	MWG	
LEW86105	H3.3	C	4	MWG	L86102
LEW87208	L3.4	B	3	MWG	
LEW87248	L3.5	A/B	2	MWG	L87208
LEW87254	LL3.5	B	3	MWG	L87208
LEW87284	L3.6	A	3	MWG	L87208
Ngawi	LL3.2/3.7	fall	444	LC	
Ngawi	LL3.2/3.7	"	512-1	AMNH	
Ngawi	LL3.2/3.7	"	2962-2	SI	
RKPA80205	H3.8	B	5	MWG	
Semarkona	LL3.0	fall	A	UCLA	
Study Butte	H3-6	find	6276-2	UNM	
TIL82408	LL3.4	B	20	MWG	
WIS91627	H3.7	B/C	4	MWG	

type = chemical group and petrographic subtype; weath = weathering category; sect = thin section number; source museums: MWG - Meteorite Working Group, SI - Smithsonian Institution, UCLA - UCLA, UNM - University of New Mexico; pairings (2nd and 3rd letters dropped) are based on this study (see Table 2 for details).

sections of the following meteorites were examined but no CMAs found: (ALH and ALHA = A; EET = E;LEW = L) A76004, A77011, A77013, A77015, A77034, A77036, A77043, A77050, A77052, A77115, A77166, A77170, A77176, A77178, A77197, A77215, A77216, A77217, A77249, A77252, A77260, A77299, A78046, A78119, A78133, A78138, A78149, A79003, A79022, A81024, A81251, A82110, A83008, A83010, A83017, A83042, A84086, A84120, A84126, A84205, A85045, A85062, A85121, A90411, Bishunpur, Chainpur, E82601, E83213, E83248, E83260, E83267, E83274, E83395, E83399, E87726, E87778, E87805, E87823, E87823, E90066, E90080, E90542, Hedjaz, Julesburg, Krymka, L85339, L85383, L85396, L85401, L85452, L86018, L86021, L86022, L86127, L86144, L86158, L86207, L86270, L86270, L86307, L86347, L86367, L86505, L86549, L88033, L8812, L88146, L88175, L88176, L88254, L88261, L88263, L88286, L88315, L88328, L88336, L88366, L88367, L88393, L88415, L88452, L88462, L88467, L88477, L88484, L88500, L88503, L88519, L88520, L88536, L88561, L88596, L88617, L88621, L88632, L88644, L88696, L88758, L88783, MAC88174, MAC88199, Manych, OTTA80301, PCA91355, Piancoldoli, Ragland, RKP86700, RKPA79008, RKA80207, RKPA80256, Sharps

3.1. H3 Chondrites

Carbide-magnetite assemblages were observed in three H3 chondrites (Study Butte, WIS91627, and RKPA80205). Only those in the Study Butte H3-6 regolith breccia have been previously described (Fredriksson et al., 1989). In all

Table 2. Pairing of CMA-bearing type-3 ordinary chondrites from Lewis Cliff and Elephant Moraine.

chondrite	type	weath	ss	pairing	ice field	ref	abundance crb	abundance mgt	carbide coh	carbide hax	km Co, wt%	tn Ni, wt%
LEW85434	L3.4	C	S1	LEW86102	l	13(2)	high	high	n.a.	n.a.	n.a.	n.a.
LEW85437	L3.4	C	S1	LEW86102	l	13(2)	high	high	n.d.	+	13-17	48-68
LEW86102	L3.4	C	S1		n	13(3)	high	high	n.d.	+	11-13	56-66
LEW86105	L3.4	C	S1	LEW86102	n	13(3)	high	high	n.a.	n.a.	n.a.	n.a.
LEW87208	L3.4	B	S3		r	12(1)	mod	mod	n.d.	+	2-25	48-61
LEW87248	L3.5	A/B	S3	LEW87208	r	12(1)	mod	mod	+	+	2-4	46-65
LEW87254	L3.5	B	S3	LEW87208	r	12(1)	mod	mod	+	+	2-25	52-64
LEW87284	L3.6	A	S3	LEW87208	r	12(3)	mod	mod	n.d.	+	1-25	47-64
EET87735	L3.4	B	S1		i	12(3)	mod	low	+	+	6-17	57-69
EET90083*	L3.5	B	S1	EET87735	i	15(2)	low	low	+	+	1-3	31-66
EET90161	L3.4	B	S1	EET87735	i	15(2)	mod	low	+	+	3-11	51-68
EET90261	L3.4	Be	S1	EET87735	i	15(2)	mod	low	+	+	3-6	55-68
EET90519	L3.6	B/Ce	S1	EET87735	i	15(2)	mod	low	+	+	n.d.	49-66
EET90628*	L3.5	A/Be	S1	EET87735	i	15(2)	mod	high	n.d.	+	n.d.	54-57

ss - shock stage; weath - weathering category; abbreviations for ice fields: n - Lower Ice Tongue, l - Upper Ice Tongue, r - Upper Walcott Neve, i - Texas Bowl. ref - references: 13(2) - Antarctic Meteorite Newsletter (13 No. 2). n.a. - not analyzed; n.d. - not detected. km - kamacite, tn - taenite, crb - carbides, mgt - magnetite, coh - cohenite, hax - haxonite. Compositional ranges are shown for kamacite and taenite.
*may represent independent falls.

three meteorites, CMA contents are minor; metal-troilite nodules are the dominant opaque assemblages. Although Study Butte is a find, the Fe-Ni metal is only slightly weathered and the troilite and carbides not appreciably affected by terrestrial alteration; magnetite grains were, however, partially replaced by secondary iron oxides. Fresh metal-troilite nodules are abundant in thin sections of both Antarctic H3 chondrites, H3.7 WIS91627, and H3.8 RKPA80205, an indication of minimal terrestrial alteration.

Study Butte has the highest abundance of CMAs among our three H3 chondrites; only a few CMAs were found in WIS91627 and RKPA80205. Carbide-magnetite assemblages are randomly distributed throughout the thin sections and occur exclusively in matrix material as polymineralic coarse-grained nodules, up to 400 μm in size, consisting of kamacite, carbides, Ni-rich (48–61 wt% Ni) taenite, troilite, and magnetite (Fig. 1a–c, Table 1). We also observed isolated carbide grains, 50–100 μm in size, which may be fragments of the polymineralic nodules, magnetite grains up 100 μm in size, and metal-troilite-magnetite nodules without carbides. Haxonite and cohenite have similar abundances to one another, although coexisting haxonite and cohenite are rare and observed in only two nodules (Fig. 1c,d). Typically, carbides either form intergrowths or show replacement textures with kamacite and Ni-rich taenite. Magnetite is preferentially concentrated in the outer zone of these inclusions where it replaces metal, troilite, and carbides (Fig. 1d); it is nearly pure in composition.

The H3 carbides are readily resolved from one another by their Ni contents (haxonite, 4.6–5.1 wt% Ni; cohenite, 1.2–1.6 wt% Ni; with the exception of one low-Ni haxonite grain in WIS91627). With the exception of two grains with Co ~0.02 wt%, the Co contents vary from 0.1–0.5 wt% (Fig. 2a,d,g). In Study Butte, the haxonite values form two clusters, with Co in cohenite similar to the higher haxonite cluster (Fig. 2a). In contrast, in RKPA80205 cohenite Co is low, <0.15 wt%, whereas haxonite values spread from 0.3–0.6 wt% (Fig. 2g). A nearly Ni- and Co-free cohenite was found in the outer part of a magnetite grain containing an angular inclusion of chromite in WIS91627 (Fig. 1f). Kamacite grains in CMAs have higher and more variable Co contents (0.5–1.4 wt%) than those in metal-troilite nodules (0.48 ± 0.09 wt% Co; Fig. 2c,f,i). The latter are in the range of kamacite compositions in CMA-free H chondrites (0.45–0.51 wt% Co; Rubin, 1990). Taenite in association with kamacite and troilite varies by a factor of 2 in Ni content (29–57 wt% Ni; Fig. 2b,e,h) and by a factor >10 in Co content (0.05–0.6 wt%); thus, these grains are far from equilibrium.

3.2. L3 Chondrites

Carbide-magnetite L3 chondrites can be divided into two types: (1) carbides are abundant, but magnetite is minor; and (2) carbides and magnetite are both abundant. The L3 chondrites from Elephant Moraine are mainly from the first group (EET90083 and EET90628 are exceptions), those from Lewis Cliff belong to the second group.

3.2.1. L3 chondrites from Elephant Moraine

Carbide-magnetite assemblages having very low magnetite contents are the dominant opaque phases in matrices of most L3 chondrites from Elephant Moraine; metal-troilite nodules are very rare (EET90083 is the only exception in that it has more abundant metal-troilite nodules). Six EET chondrites contain CMAs (Table 1); two of them (EET90161 and EET90261) have been previously paired (Grossman, 1994). Although all are moderately weathered (weathering categories vary from A/B to B/C), alteration of the CMAs is minor to negligible. This resistance to terrestrial weathering further enhances the value of CMAs as recorders of asteroidal or nebular alteration conditions.

Carbide-magnetite assemblages occur as irregularly-shaped or rounded nodules, 200–300 μm in size, in matrix

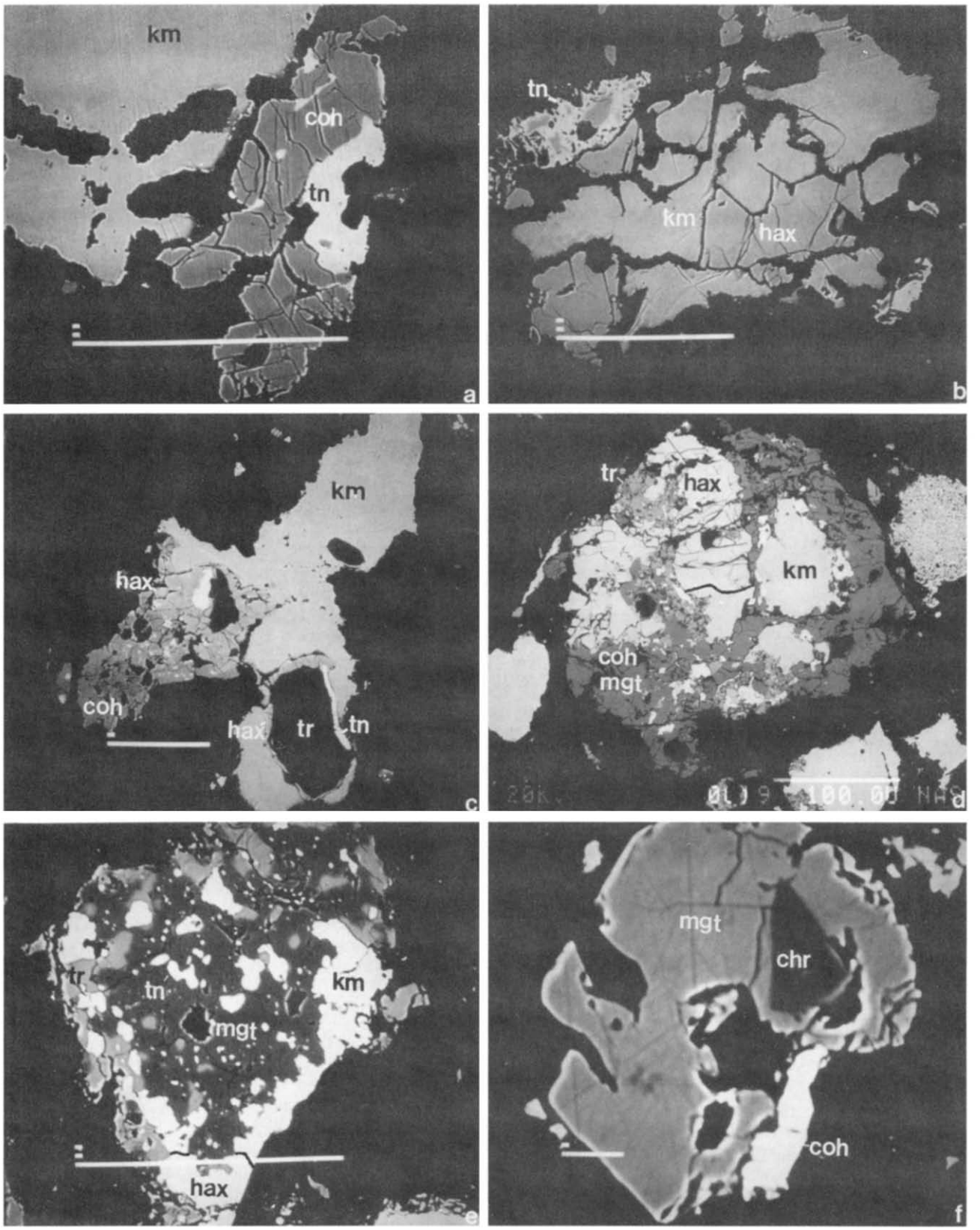

Fig. 1. Back-scattered electron images of carbide-magnetite assemblages in the H3-6 Study Butte (a–c), H3.8 RKPA80205 (d) and H3.7 WIS91627 (e,f). (a) Inclusion 8 consists of kamacite, cohenite, and Ni-rich taenite. (b) Inclusion 12 consists of kamacite, haxonite, and Ni-rich taenite. Haxonite forms intergrowths with kamacite and irregularly-shaped inclusions in Ni-rich taenite. (c) Inclusion 18 consists of kamacite, troilite (black inclusions in

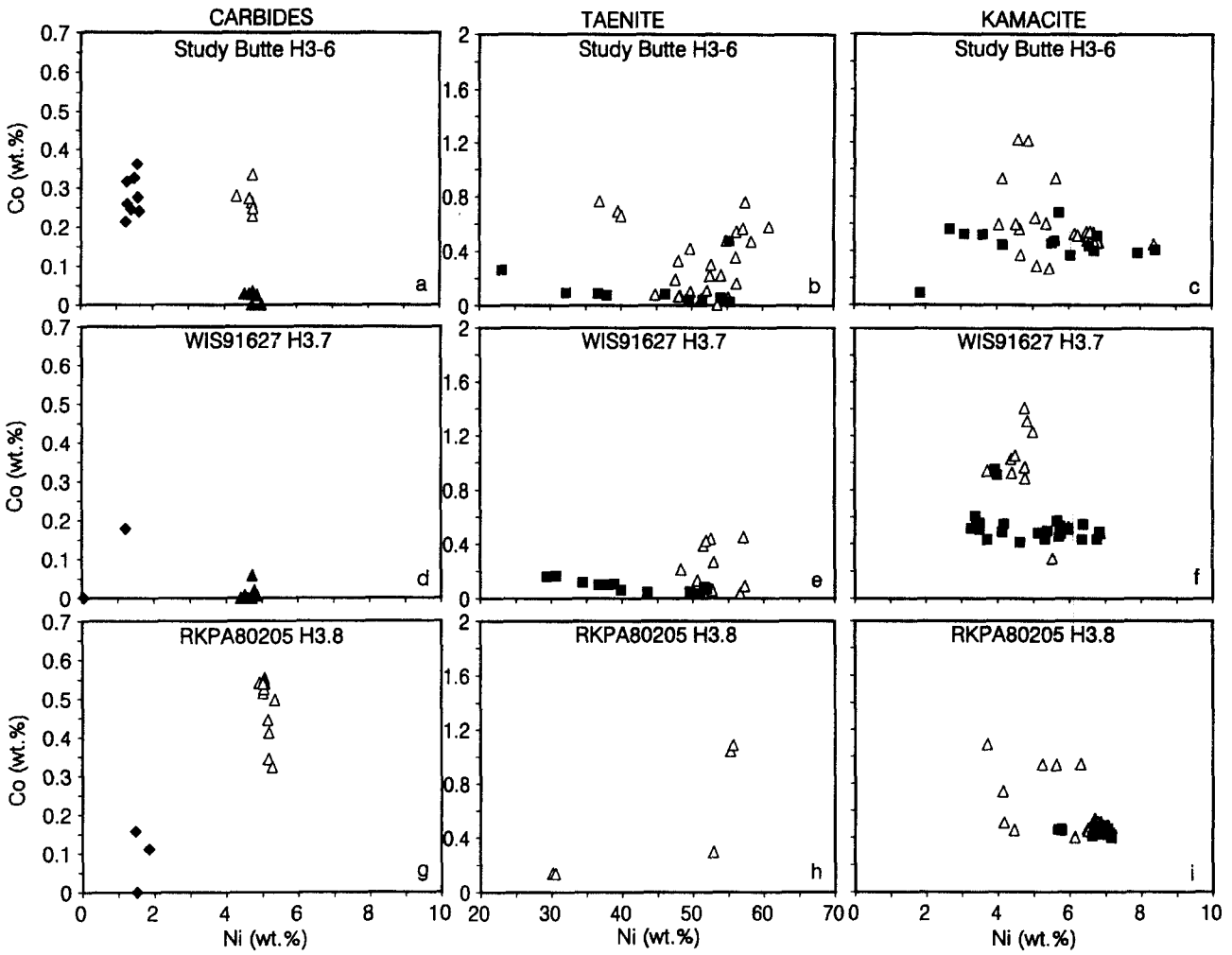

Fig. 2. Compositions of carbides (a,d,g), taenite (b,e,h), and kamacite (c,f,i) in H3 chondrites. Cohenite, high-Ni, and low-Ni haxonite are shown by diamonds, open and filled triangles, respectively. Kamacite and taenite in association with carbides and/or magnetite are shown by triangles, without carbides or magnetite by filled squares.

material or as rounded nodules in chondrule rims, and inside FeO-poor chondrules. Carbide-magnetite nodules inside chondrules occasionally coexist with metal-troilite nodules; the former occur in peripheral zones (see Fig. 5c), the latter are more common in chondrule cores or as inclusions in olivine and pyroxene phenocrysts. Nearly monomineralic 50–100 μm aggregates of small carbide grains were observed in the interchondrule matrix of EET87735, EET90161, and EET90519. Most carbide-bearing nodules outside chondrules are surrounded by matrix-like material and a few have an additional outer layer consisting of coarse-grained intergrowths of Ni-rich taenite and carbides. Thin carbide veins with negligible magnetite connecting with carbide-magnetite nodules and crosscutting matrix-like material occur in EET90628 and appear similar to those described in Semarkona (Hutchison et al., 1987).

kamacite), Ni-rich taenite (white), haxonite (light-gray), and cohenite (dark-gray). Haxonite forms intergrowths with kamacite and a rim around the largest troilite inclusion (bottom right). Cohenite forms intergrowths with haxonite (bottom left). Both carbides contain abundant inclusions of Ni-rich taenite. Magnetite replaces kamacite and carbides in the outer parts of the inclusions 8, 12, and 18; it appears black in a–c. (d) Inclusion 1 consists of magnetite (dark-gray) replacing kamacite, haxonite, cohenite, Ni-rich taenite (all 4 phases are white), and troilite (light-gray). Haxonite forms an intergrowth with kamacite in the center of the inclusion (the black line is the boundary between two minerals). (e) Inclusion 21 has a magnetite-rich core with abundant inclusions of Ni-rich taenite (white) and troilite (light-gray); its outer part consists of troilite, kamacite, and haxonite (bottom center). (f) An intergrowth of cohenite (white) and magnetite (gray); the latter contains an angular chromite inclusion (black). White scale bars in a–e are 100 μm, scale bar in f is 10 μm. chr—chromite, coh—cohenite, hax—haxonite, km—kamacite, mgt—magnetite, tr—troilite, tn—Ni-rich taenite.

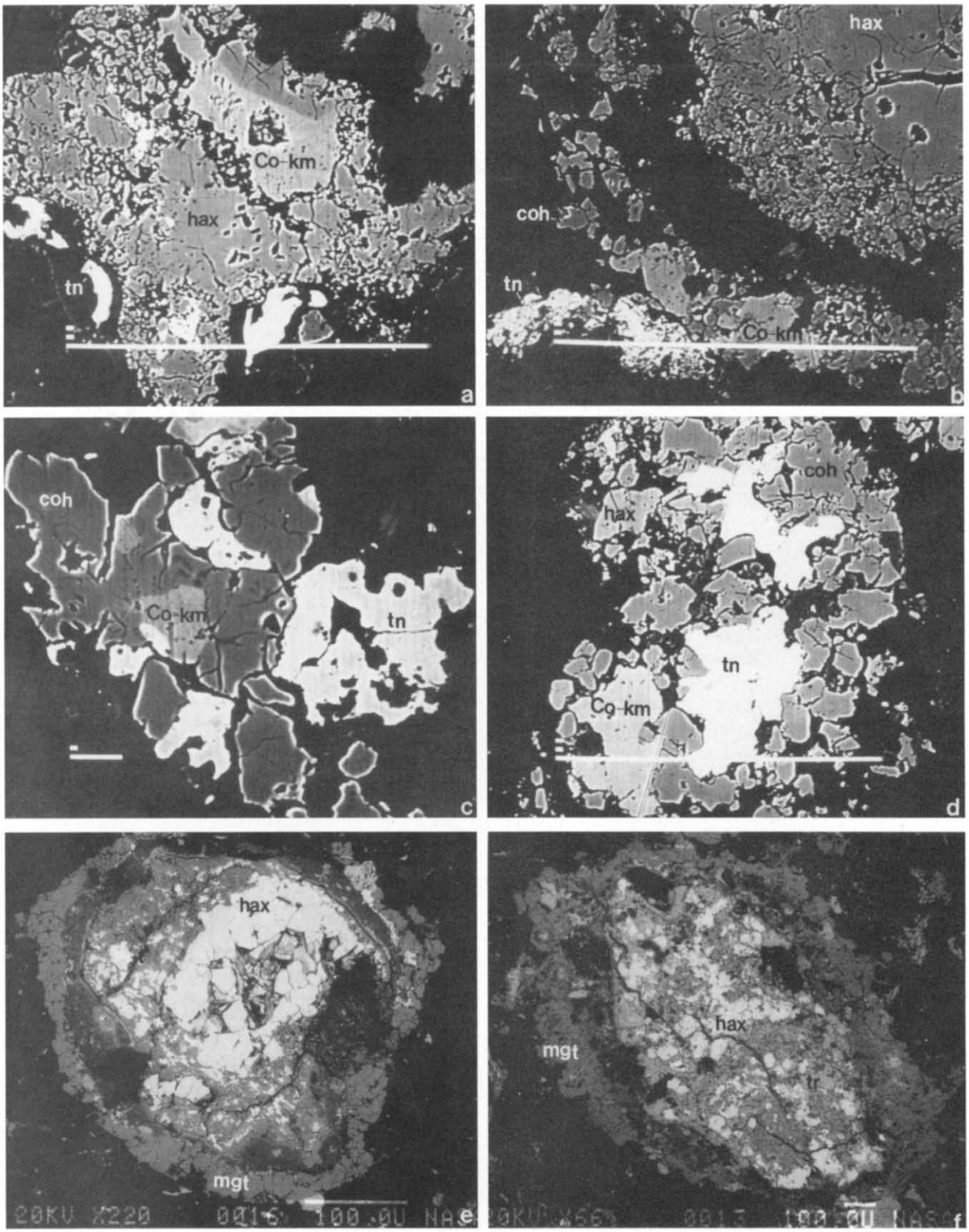

Fig. 3. Back-scattered electron images of carbide-magnetite assemblages in the L3.4 EET90161 (a–d) and L3.5 EET90628 (e,f). (a) Inclusion 15a consists of haxonite with inclusions of Ni-rich taenite and Co-rich kamacite. (b) Inclusion 3 has a nearly monomineralic haxonite core (top right); it is surrounded by a polymineralic rim consisting of haxonite, cohenite, Co-rich kamacite, and Ni-rich taenite. (c) Inclusion 16 has a coarse-grained texture; it consists

There are two textural types of carbide-bearing inclusions in EET87735, EET90161, and EET90519 that occur in close proximity: coarse-grained polymineralic inclusions and fine-grained nearly monomineralic inclusions (Fig. 3a–d). The coarse-grained inclusions consist of carbides, Co-rich kamacite, Ni-rich taenite, and troilite (Fig. 3c,d). Most fine-grained inclusions have a compact core and a porous outer zone and consist mainly of carbides with minor Co-rich kamacite and Ni-rich taenite and rare magnetite (Fig. 3a,b). EET90628 contains mainly fine-grained carbide-bearing nodules which are partly replaced by magnetite (Fig. 3e,f). The only CMAs observed on EET90083 are fragments of fine-grained carbide-magnetite inclusions.

Haxonite and cohenite are compositionally variable (4.6–5.3 wt% Ni, ~0.25 wt% Co and 1.9–2.2 wt% Ni, 0.4–0.9 wt% Co, respectively) and are equally abundant in EET87735, EET90161, and EET90519 (Fig. 4a,d,g). In contrast, haxonite grains with relatively high Ni (~5.3 wt%) and Co (~0.5 wt%) contents are dominant in EET90628 (Fig. 4m). A few haxonite grains have anomalously-high Ni contents (>6 wt%). Kamacite in association with carbides has very high Co content (up to 18 wt%); taenite is Ni- and Co-rich (>50 wt% and up to 2.5 wt%, respectively) (Fig. 4b,e,h,k,n). Kamacite in metal-troilite nodules in EET90083 have low, L-like Co contents; taenite is Ni-poor (Fig. 4c,f,i,l,o).

TEM observations of the matrix of L3.4 EET90161 show that olivine and pyroxene have been partially replaced by Ca-Na-K-Fe-rich saponite. This phase was identified on the basis of its flaky morphology, basal lattice fringes varying from 0.99–1.02 nm, and composition, which averaged to $(K_{0.99}Ca_{0.38}Na_{0.44})(Mg_{3.91}Fe_{2.11})(Si_{7.16}Al_{0.5}Fe_{0.34})O_{20}(OH)_4$-$8H_2O$ (oxygen and water assumed by formula stoichiometry). This composition compares favorably with that obtained for Semarkona smectite by Hutchison et al. (1987), where Fe was also required to be in tetrahedral coordination. However, the high K content of EET90161 saponite is more reminiscent of that noted from Bishunpur (Alexander et al., 1989).

3.2.2. *L3 chondrites from Lewis Cliff*

Eight type-3 OC from Lewis Cliff, previously classified as H3, L3, or LL3, contain CMAs (Table 1) and appear to represent only two L3 falls. Based on similarities in mineralogy, chemistry, and abundances of CMAs, textures and degree of weathering, these chondrites are divided into (1) LEW85434, LEW85437, LEW86102, and LEW86105, and (2) LEW87208, LEW87248, LEW87254, and LEW87284. LEW85434 and LEW85437 and LEW86102 and LEW86105 have been previously paired and classified as L3.4 and H3.3, respectively (Grossman, 1994). Here the meteorites within each cluster are classified (or reclassified) as L3 chondrites and are probably paired (see Table 2 and Appendix A).

3.2.3. *LEW85434, LEW85437, LEW86102, and LEW86105*

Carbide-magnetite assemblages are abundant in these meteorites and typically occur as rounded nodules, 200–600 μm in apparent diameter, outside chondrules. The majority have a fine-grained texture and are mineralogically zoned (Fig. 5a). Their cores consist of troilite and magnetite with irregularly shaped inclusions of Ni-rich taenite, haxonite, and Co-rich kamacite, indicating a reactional origin of the magnetite. Haxonite occurs as irregularly-shaped inclusions in Ni-rich taenite or forms intergrowths with Ni-rich taenite. Nodule cores are surrounded by a thin silicate inner rim and a porous or compact outer carbide rim. The carbide rim is typically overgrown by subhedral grains of magnetite without visible inclusions of carbides or metal. Isolated magnetite grains with relatively uniform sizes and morphologies are common throughout matrix material as well. In some cases, fine-grained magnetite fills interstitial areas between chondrule fragments and individual silicate grains, which probably indicates that the growth of magnetite postdates fragmentation and agglomeration (Fig. 5f). One radial pyroxene chondrule in LEW85437 contains a magnetite-haxonite-metal nodule with trapped silicates compositionally and texturally similar to those in the host chondrule (Fig. 5c,d). These textural observations suggest incomplete metal-silicate separation during chondrule formation and subsequent replacement of the metal by haxonite, magnetite, Ni-rich taenite, and Co-rich kamacite. Several carbide-magnetite nodules outside chondrules contain silicate inclusions with microporhyritic textures indicating that these nodules were completely expelled from chondrules or were melted with minor amounts of silicates, and, hence, are opaque-rich chondrules. Alexander et al. (1989) described low-Ca pyroxene inclusions with twinned monoclinic structures requiring high temperature and rapid cooling. Alexander et al. (1989) also concluded that the original nodules were expelled from chondrules. In some cases, carbide-magnetite nodules contain high abundances of tiny (<1 μm) silicate inclusions randomly distributed in magnetite and Ni-rich taenite cores (Fig. 5e). The presence of texturally similar metal-troilite nodules with silicate dust in the CMA-free type-3 OC (e.g., Perron et al., 1990) indicates that carbide-magnetite nodules with silicate dust formed by replacement of the dusty metal-sulfide nodules.

Haxonite (4.8 ± 0.4 wt% Ni, 0.42 ± 0.05 wt% Co) is the dominant carbide phase in LEW85434 and LEW86102

of cohenite, Ni-rich taenite, and Co-rich kamacite. (d) Inclusion 15c consists of haxonite, cohenite, Co-rich kamacite, and Ni-rich taenite. (e) Inclusion 3 is mineralogically zoned. Its core consists of fine-grained haxonite partly replaced by magnetite. The core is surrounded by a matrix-like rim (nearly black) and additional magnetite rim. (f) Inclusion 1 has a troilite-silicate-haxonite core; it is surrounded by a matrix-like rim (black) and magnetite rim. Scale bars in a,b,d–f are 100 μm, scale bar in c is 10 μm. coh—cohenite, hax—haxonite, Co-km—Co-rich kamacite, mgt—magnetite, tr—troilite, tn—Ni-rich taenite.

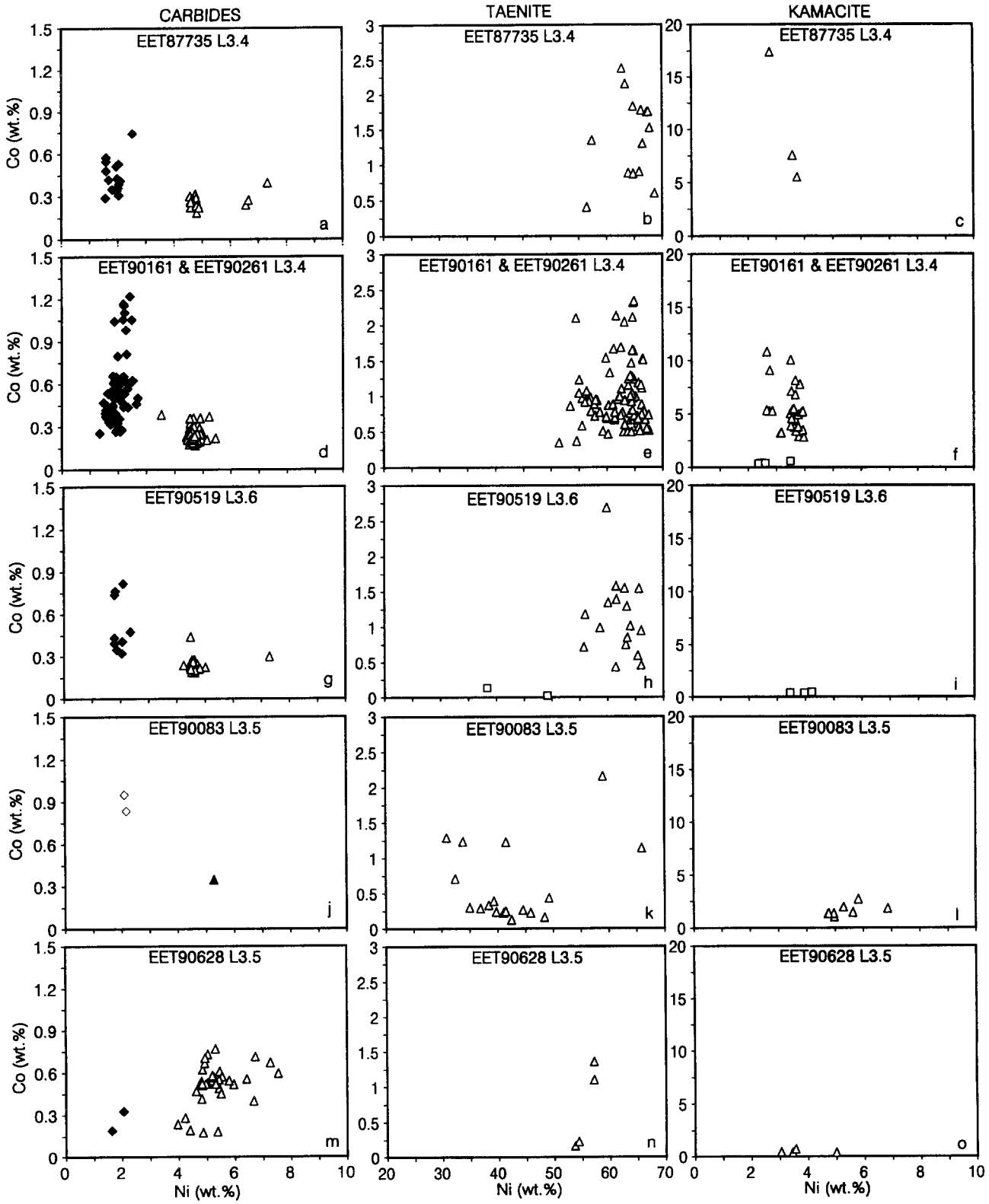

Fig. 4. Compositions of carbides (a,d,g,j,m), taenite (b,e,h,k,n), and kamacite (c,f,i,l,o) in L3 chondrites from Elephant Moraine. Kamacite and taenite inside chondrules not associated with carbides and/or magnetite are shown by open squares.

(Fig. 6a). Four carbide grains have very low Fe contents (<84 wt%); these analyses are from porous fine-grained carbide rims and possibly reflect analytical problems. Kamacite in CMA is Co-rich (Fig. 6c); taenite has high Ni (>55 wt%) and Co (0.5–2 wt%) contents (Fig. 6b). Kamacite grains in magnetite-carbide-free nodules inside chondrules have low Co contents. Metal-troilite nodules were not observed outside of chondrules.

3.2.4. LEW87208, LEW87248, LEW87254, and LEW87284

Carbide-magnetite assemblages are common in these meteorites but less abundant and texturally different from those described above. Typically these assemblages occur as ellipsoidal nodules in matrix and chondrule rims. CMAs inside chondrules are rare (Fig. 7b) and commonly coexist with metal-sulfide nodules. Most of the CMAs have granular textures and consist mainly of troilite and kamacite with accessory magnetite, carbides, and Ni-rich taenite (Fig. 7a). Magnetite replaces metal and troilite. Individual magnetite grains, up to 100 μm in size, also occur in matrix. Two unusual carbide-bearing nodules were found in LEW87284 and LEW87248 (Fig. 7c,d). The LEW87284 nodule consists of coarse-grained intergrowths of Ni-rich taenite and haxonite, and minor Co-rich kamacite, magnetite, and troilite, with interstitial fine-grained cohenite embedded in silicate material. The LEW87248 nodule consists of polycrystalline cohenite with an irregularly-shaped inclusion of Ni-rich taenite and a rounded silicate inclusion.

As in other L3 chondrites from Lewis Cliff described above, haxonite (~4.7 wt% Ni, ~0.5 wt% Co) is the dominant carbide phase and cohenite (1.9–2.1 wt% Ni, ~0.4 wt% Co) is minor (Fig. 6d,g,j,m). Kamacite varies significantly in composition; no kamacite grains with Co > 4 wt% were found in LEW87248 (Fig. 6f,i,l,o). Taenite in CMAs has high Ni (>50 wt%) and variable Co content (0.05–1.7 wt%; Fig. 6e,h,k,n).

3.3. LL3 Chondrites

Four LL3 chondrites were found to contain CMAs which consist of magnetite, troilite, Ni-rich sulfide, carbides, Ni-rich taenite, and Co-rich kamacite (Table 1, Figs. 8, 9, 10). Carbide-magnetite assemblages are most abundant in Semarkona; metal-troilite nodules are nearly absent in the single thin section studied. Examination of three thin sections of Ngawi and two thin sections of ALHA77278 (both meteorites are breccias) showed that the abundance of metal-troilite nodules and CMAs varies significantly within these meteorites, which is possibly related to late-stage brecciation.

The Ni-rich sulfides (Fig. 10), similar to those previously observed in Semarkona and chondritic IDPs, lie mainly between the composition of troilite (which will only accomodate <2 at% Ni) and pentlandite (properly >25 at% Ni). Although it may be that these sulfide grains represent intergrowths between these two endmember phases, some workers have suggested that these could instead represent a poorly-characterized Fe-Ni sulfide phase that can have a large range in Ni contents (Alexander et al., 1989; Zolensky and Thomas, 1995).

The abundance of magnetite in the CMAs of LL3 chondrites varies from ~0% to ~100% (Fig. 8a–d). The CMAs occur as coarse-grained, irregularly-shaped nodules in matrix and as nodules in chondrules and chondrule rims. Isolated carbides in matrix material form large grains (up to 75 μm in size), and thin (1–5 μm width) veins cross-cutting matrix material (Fig. 8b–d). Carbide grains in CMAs appear to be replaced by magnetite. Individual magnetite grains, up to 200 μm in size, and fine-grained magnetite aggregates cementing silicate grains are also observed in the matrix of Semarkona, Ngawi, and ALHA77278.

Carbides show a wide range in composition (1–14 wt% Ni, 0.15–1.3 wt% Co); although there are modes at ~1.5 (cohenite) and ~4.5 wt% Ni (haxonite), there is no hiatus in Ni contents (Fig. 9a,d,g,j). Taenite grains in CMAs have high Ni and Co contents (Fig. 9b,e,h,k). Low Ni metal in CMAs is Co-rich (Ngawi and ALHA77278) or absent (Semarkona and TIL82408) (Fig. 9c,f,i).

Scott (1971) originally described the high-Ni carbide, haxonite, in iron meteorites. The structure of this mineral had never been investigated. Accordingly, we chose one high-Ni carbide (5.6 wt%) in Semarkona, presumed to be haxonite on account of the high Ni content and isotropy, for structural characterization by Laue X-ray techniques. The composition of this carbide, determined by electron microprobe, was 88.2 wt% Fe, 5.6 Ni, 0.57 Co, and 5.7 C by difference. The X-ray pattern obtained from the exact location of the microprobe analyses indicated the space group Fm3m with a unit cell dimension of 1.078 nm, in good agreement with the value of 1.055 nm reported by Scott (1971). A structure refinement (including metal site occupancy determination) of this haxonite grain is in progress.

Summarizing the petrographic observations, CMAs occur in matrix, chondrules, and chondrule rims in several H3, L3, and LL3 chondrites. Although the majority of carbide-bearing type-3 OC contain both carbides and magnetite, relative mineral abundances vary in a broad range. There are two types of carbide-magnetite-bearing L3 chondrites: those where carbides and magnetite are both abundant and those with abundant carbides but only minor magnetite. Magnetite typically replaces metal, troilite, and carbides. In some cases, the relationships between carbides and magnetite are less clear. Metal-troilite nodules are rare in matrices of carbide-magnetite OCs, but adjacent metal-troilite nodules and CMAs are common in brecciated chondrites (e.g., Study Butte, Ngawi, ALHA77278). Carbide-magnetite nodules inside chondrules coexist with metal-troilite nodules; the formers are typically observed in the outer portions of chondrules, the latters occur in chondrule cores or as inclusions in olivine or pyroxene phenocrysts. Carbide-magnetite nodules outside chondrules are mineralogically and texturally similar to those inside chondrules; they occasionally contain silicate inclusions having textures indicating that they experienced melting. Fe-Ni metal in carbide-magnetite-bearing chondrites consists mainly of high-Ni taenite and Co-rich kamacite. Textural and mineralogical observations indicate that carbide-magnetite nodules were completely or incompletely

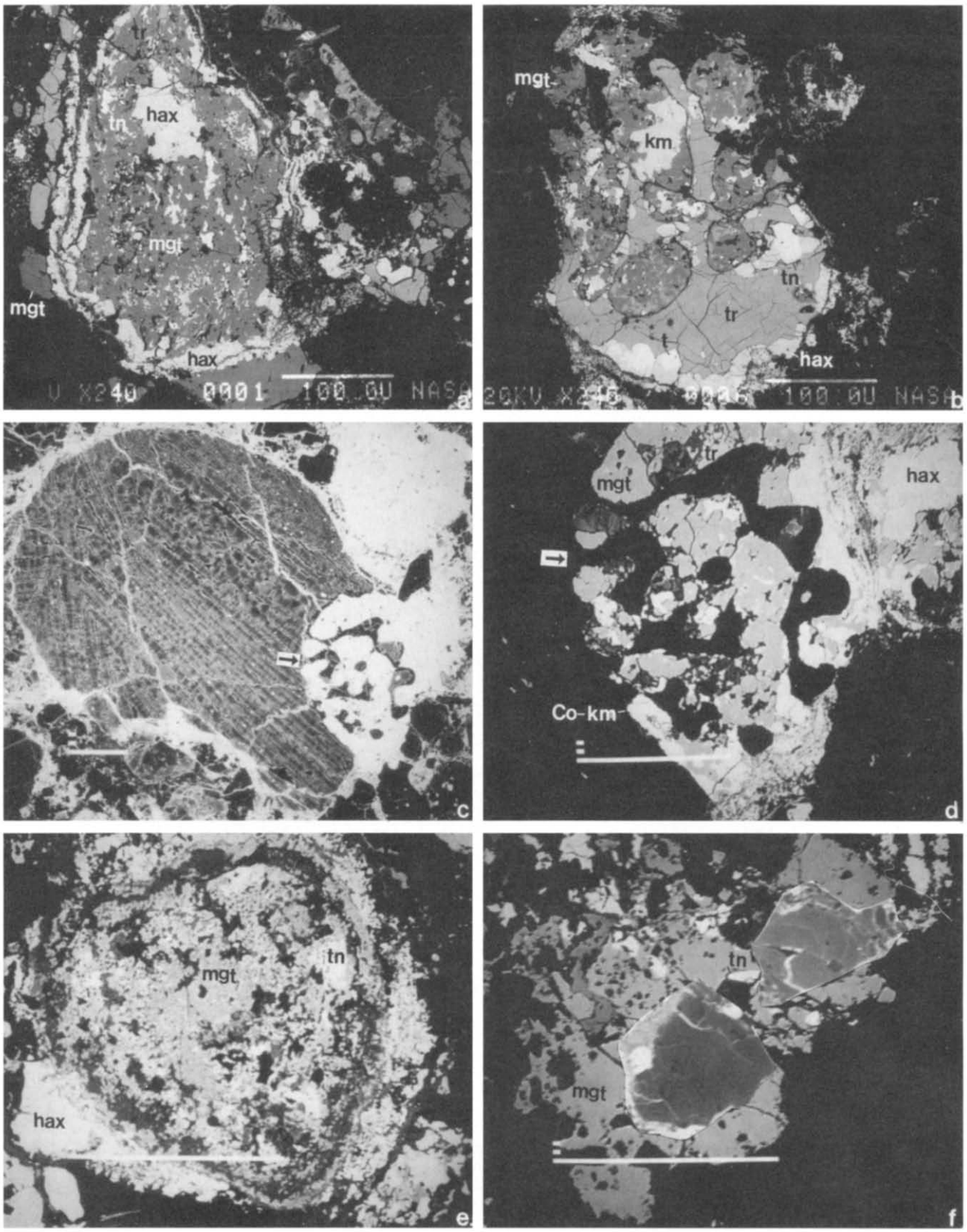

Fig. 5. Back-scattered electron images of carbide-magnetite assemblages in the L3.4 LEW86102 (a,b) and LEW85437 (c–f). (a) Inclusion 6 is mineralogically zoned. Its core consists of fine-grained magnetite replacing Ni-rich taenite, haxonite, and troilite. The core is surrounded by two haxonite rims separated by a thin silicate layer (black). The outer carbide rim is overgrown by subhedral magnetite grains. (b) Inclusion 1 consists mainly of fine-

expelled from chondrules as metal-troilite nodules and were later replaced by carbides and magnetite; the residual metal became enriched in Ni (taenite) and Co (kamacite).

4. DISCUSSION

4.1. Origin of Carbide-Magnetite Assemblages

4.1.1. Carbide-magnetite assemblages are not the result of weathering

Although the majority of carbide-magnetite-bearing chondrites are Antarctic finds, none of the CMA carbides and, at most, minor fractions of the magnetite formed by terrestrial oxidation. Carbide-magnetite assemblages in type-3 OCs from Antarctica have similar textures, mineralogy, and chemistry to those in Semarkona and Ngawi, which are falls. Magnetite and carbides are absent in most Antarctic type-3 OC. Carbides are highly resistant to low-temperature terrestrial oxidation (Alexander et al., 1989). Some CMAs show evidence of brecciation (e.g., EET90083) and imply that they formed before the extraterrestrial brecciation event. We exclude the possibility that appreciable magnetite in Antarctic OCs formed during terrestrial alteration.

4.1.2. Key features of carbide-magnetite assemblages to be modeled

The petrographic data are often ambiguous with regard to the sequence in which minerals formed in the CMAs. With this caveat in mind, we will make the following tentative generalizations that will then serve as constraints on possible models. The key petrographic features common to the CMAs in low type-3 members of all three OC groups are that the carbides (cohenite and haxonite) are generally associated with metal, either filling embayments in metal or containing inclusions of high-Ni taenite and Co-rich kamacite suggesting replacement of metal by carbide. In other cases, the carbides occupy similar relationships to sulfides (Figs. 5b, 7a,d). However, since sulfides are commonly associated with metal, it is possible (and, we think, probable) that these carbides also mainly formed by replacing metal. The presence of unaltered metal-troilite nodules in chondrule cores or as inclusions in olivine and pyroxene phenocrysts and carbide-magnetite nodules in the outer portions of chondrules (A. Rubin, pers. commun., 1995; this study) supports this conclusion.

It seems important that magnetite-rich type-3 OCs without carbides have not been found. This probably indicates that formation of carbides and magnetite in OCs are closely related (in time and space) processes. Magnetite, which is present in a variable ratio to carbides, tends to occupy replacement relationships with either metal or carbides (Figs. 1d, 3e, 5a, 8a); in some cases, textural relationships between carbides and magnetite are less clear. In about half the cases magnetite is a minor component of compact CMAs. Magnetite and carbides also form detached massive shells (or shell fragments) outside the compact carbide-metal-sulfide-magnetite cores (Figs. 3e,f,5a) or fine-grained regions associated with Ni-rich taenite (Fig. 5f). These observations may indicate multistage and sequential formation of magnetite and carbides, with most magnetite forming after formation of carbides. Alternatively, the outer nearly monomineralic shells may have formed during replacement of metal by magnetite in locations such as chondrules which could not accomodate the resulting volume increase; the excess Fe then diffused away to open sites where massive magnetite shells could grow (C. M. O. Alexander, pers. commun., 1996). The absence of magnetite in some of carbide-magnetite OCs could be a result of variations in fluid compositions.

There are several textural observations suggesting that formation of CMAs occurred in an asteroidal environment (thermodynamic reasons for asteroidal formation are discussed in Section 4.1.5.): (1) Presence of CMAs in chondrules, chondrule rims, and matrix materials indicate that formation of CMAs is a late stage, low-temperature process (after chondrule formation and accretion of fine-grained rims (Fig. 3e,f) below condensation temperature of troilite) that affected all major OC components; (2) occurrence of massive magnetite grains occupying interstitial areas between chondrule fragments with various textures and compositions (Fig. 5f) indicates that crystallization of magnetite must have taken place after agglomeration of previously fragmented chondrules; (3) Presence of carbide-magnetite veins cross-cutting chondrule rims and extending into the matrices of several carbide-magnetite type-3 OCs suggests that these veins formed in asteroids; (4) Carbide-magnetite assemblages are observed in only about 10% of the type-3 OCs we examined. If carbides and magnetite formed in the solar nebula, it would imply local compositional variations of the low-temperature nebula gas at the accretional regions of H, L, and LL chondrites and rapid accretion of altered materials in order to prevent mixing with unaltered, carbide-magnetite-free OCs. If carbides and magnetite formed in asteroids, it would imply that the carbide-magnetite chondrites formed in separate parent bodies or that CMA formation sites were heterogeneously distributed in the main OC parent bodies. The latter is supported by the fact that coexisting carbide-

grained troilite. Intergrowths of haxonite and Ni-rich taenite occur in the peripheral zone of the inclusion (bottom center). Rounded nodules in troilite consists of magnetite, Ni-rich taenite, and troilite; one nodule contains an inclusion of Co-rich kamacite (marked as km). (c,d) A radial-pyroxene chondrule containing an opaque nodule with trapped silicate droplets (bottom right). The opaque phases in nodule consists of magnetite, Co-rich kamacite, and haxonite. (e) Inclusion 19 has a fine-grained core consisting of magnetite and Ni-rich taenite; both minerals have high abundance of tiny silicate inclusions (black). The core is surrounded by a matrix-like rim (black) and haxonite rim. (f) Fine-grained magnetite with small inclusions of Ni-rich taenite (white), angular mineral fragments (black), and two chondrule fragments (center and top right). Scale bars in a–f are 100 μm. Chr—chromite, coh—cohenite, hax—haxonite, Co-km—Co-rich kamacite, mgt—magnetite, tr—troilite, tn—Ni-rich taenite.

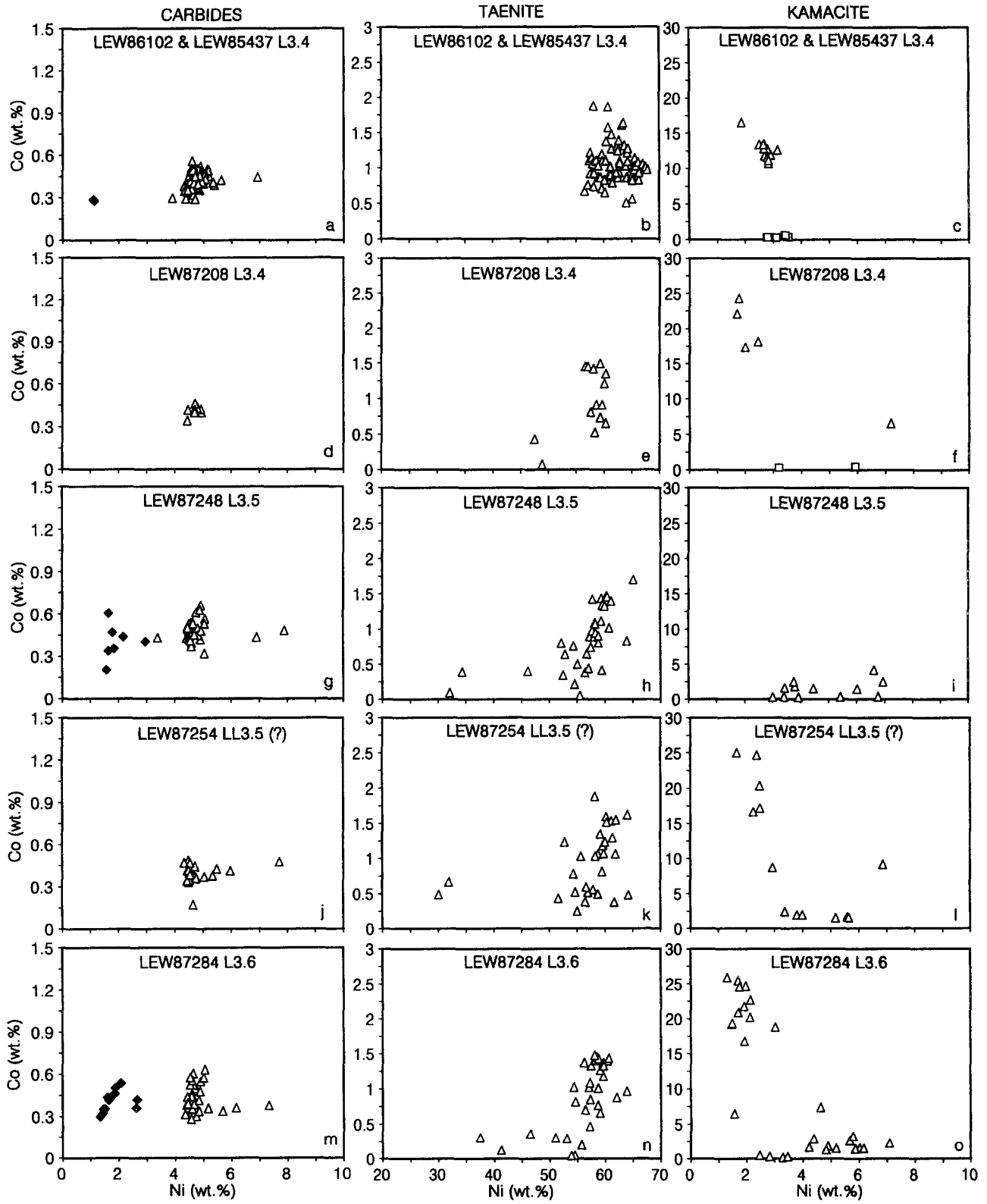

Fig. 6. Compositions of carbides (a,d,g,j,m), taenite (b,e,h,k,n), and kamacite (c,f,i,l,o) in L3 chondrites from Lewis Cliff. Kamacite and taenite inside chondrules not associated with carbides and/or magnetite are shown by open squares.

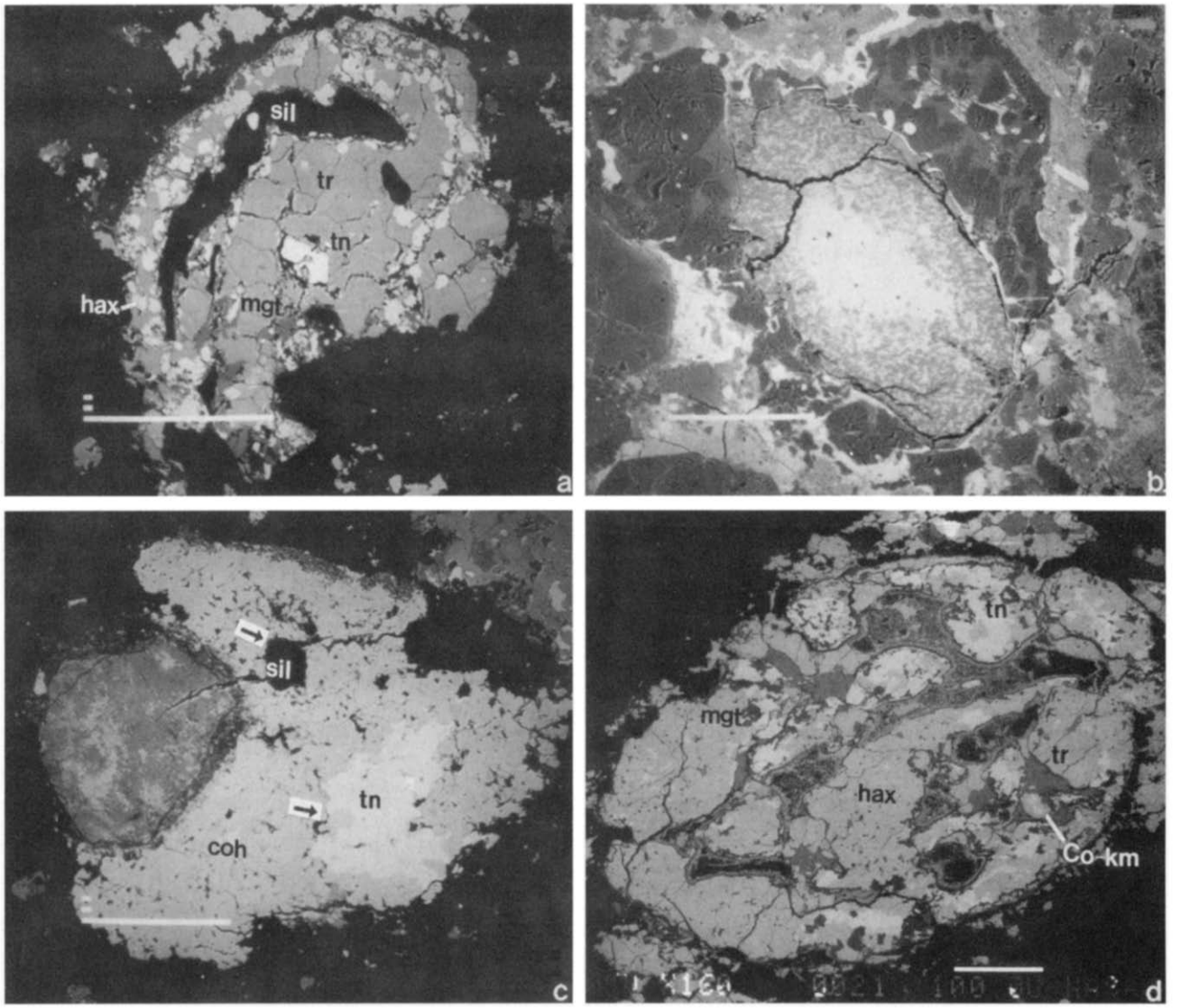

Fig. 7. Back-scattered electron images of carbide-magnetite assemblages in the L3.5 LEW87248 (a–c) and L3.6 LEW87284 (d). (a) Inclusion 7 consists mainly of troilite, Ni-rich taenite, and haxonite. Magnetite (dark-gray) replaces troilite, haxonite, and Ni-rich taenite. Two rounded silicate inclusions (black) occur in the center of the nodule. (b) A porphyritic olivine chondrule containing a large opaque nodule consisting of carbide (white) replaced by magnetite (gray). (c) Inclusion 10 consists mainly of fine-grained cohenite. An irregularly-shaped inclusion of Ni-rich taenite and rounded silicate inclusion (black) occur in the center of the cohenite nodule. A polymineralic fine-grained nodule consisting of troilite, magnetite, and carbide attached to nodule 10 (center left). (d) An ellipsoidal nodule 1 consists of coarse-grained intergrowths of Ni-rich taenite and haxonite; magnetite, troilite, and Co-rich kamacite are minor. Some areas (black) in the center of the nodule consist of a fine-grained mixture of silicate and carbide grains. Scale bars in a–d are 100 μm. coh—cohenite, hax—haxonite, Co-km—Co-rich kamacite, mgt—magnetite, sil—silicate, tr—troilite, tn—Ni-rich taenite.

magnetite and metal-sulfide nodules are commonly observed in brecciated OCs (e.g., Ngawi, ALHA77278). Heterogeneities within an asteroid could result during volatile transport along zones with various fluid permeability. Although we can not completely exclude nebular scenario, asteroidal formation of CMAs seems more realistic.

We interpret the absence or low abundance of CMAs in petrographic type >3.4 (some, perhaps all, of our samples classified >3.4 appear to be <3.4) to indicate (1) that the supply of reactants was exhausted by the time parent-body regions were thermally altered to higher petrographic grades, and (2) that CMAs formed at low temperatures were destroyed when parent bodies were heated to higher temperatures.

4.1.3. Possible sources of C and O

There is strong textural and mineralogical evidence that the CMAs formed after chondrule formation by replacement of metal-troilite nodules at relatively low temperatures (be-

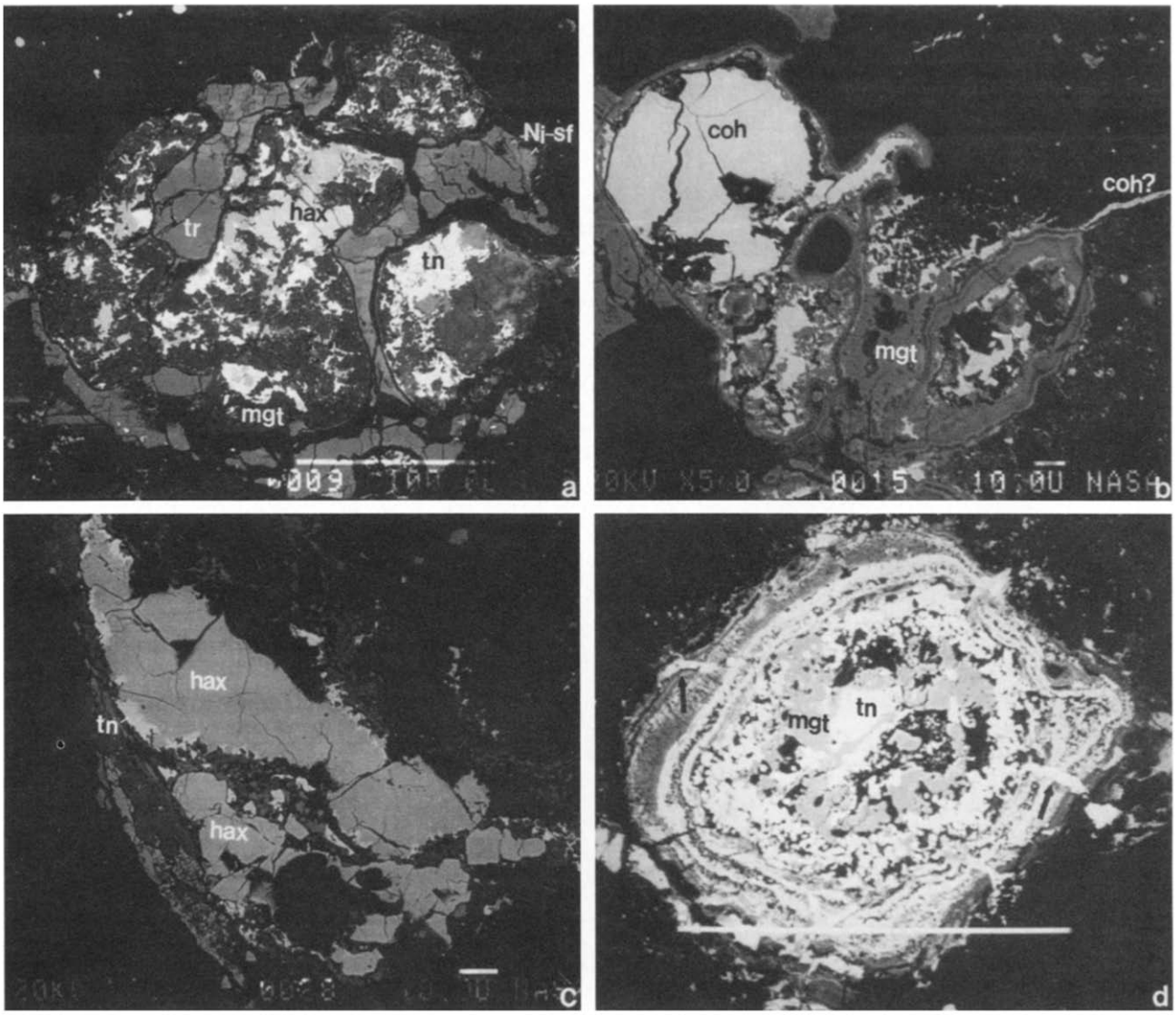

Fig. 8. Back-scattered electron images of carbide-magnetite assemblages in the LL3.0 Semarkona (a,b), LL3.2/3.7 Ngawi (c), and LL3.1/3.5 TIL82408 (d). (a) A polymineralic nodule 10 consisting of intergrowths of troilite with Ni-rich sulfide (gray) and magnetite replacing haxonite and Ni-rich taenite. (b) Microcrystalline cohenite grain partly replaced by magnetite and carbide veins crossing through matrix-like material (black). (c) Fine-grained haxonite. Haxonite grains at the bottom are homogeneous (5.9 wt% Ni, 0.66 wt% Co), those at the top (5.0 wt% Ni, 0.29 wt% Co) have rims and abundant inclusions of Ni-rich taenite (light-gray). (d) Nodule 4 has a fine-grained core consisting of magnetite with small inclusions of Ni-rich taenite and several carbide rims separated by matrix-like material. Several thin carbide veins (marked by arrows) crosscut the outer carbide layers. Scale bars in (a) and (d) are 100 μm; scale bars in (b) and (c) are 10 μm. coh—cohenite, hax—haxonite, mgt—magnetite, tr—troilite, tn—Ni-rich taenite.

low condensation temperatures of troilite (<700 K; e.g., Fig. 5b). In the low-temperature ($T < 500$ K) solar nebula, there are two main sources of O (CO(g) and H_2O(g)), one major gaseous source of C (CO(g)) and two possible minor solid sources (C and condensed hydrocarbons). Assuming equilibrium, only at temperatures below 400 K does CO_2 become more abundant than CO; however, under these conditions, CH_4 is the main gaseous form of C. In asteroidal bodies the chief source of O is probably H_2O present as water of hydration (Wasson and Krot, 1994) or as ice (McSween and Labotka, 1993). The chief source of parent-body C is likely to be solid hydrocarbons or graphite; CO is not expected to be adsorbed or to be trapped in sufficient quantities to produce large-scale alteration effects during diagenesis. Under equilibrium conditions, pCO_2/pCO is <0.1 if metallic Fe is present in the parent body.

4.1.4. Thermodynamics calculations; relative stability of cohenite and haxonite

Our modeling approach is to calculate equilibrium relationships using Gibbs-free-energy data from JANAF (1985) and,

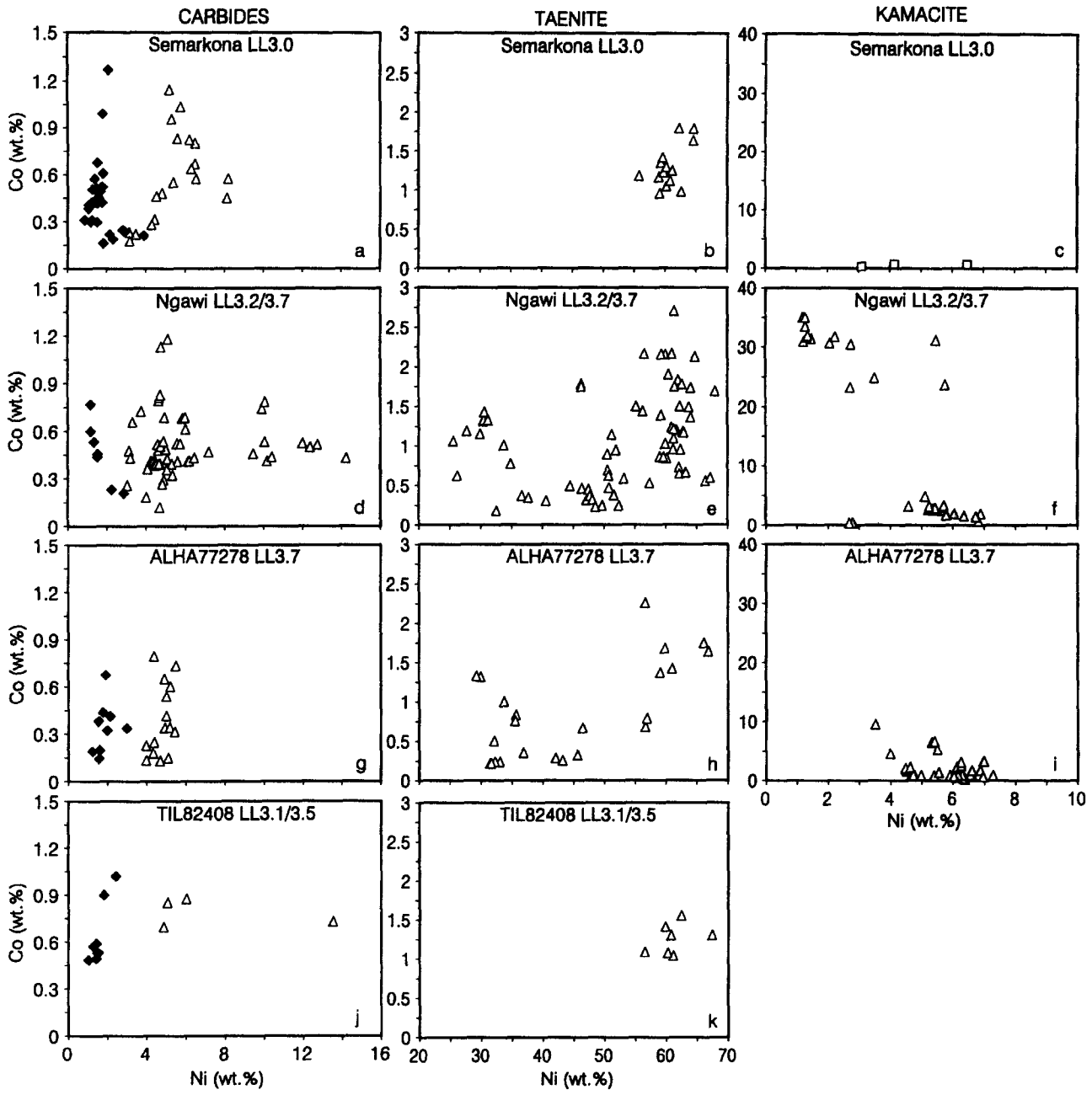

Fig. 9. Compositions of carbides (a, d, g, j), taenite (b, e, h, k), and kamacite (c, f, i) in LL3 chondrites. Kamacite grains inside chondrules not associated with carbides and/or magnetite are shown by open squares.

for cohenite, Robie et al. (1978). Solar abundance data are from Anders and Grevesse (1989); the solar pH_2/pH_2O ratio was rounded up to 1500. We also examined the possibility that kinetic factors could lead to the metastable formation of some phases. Cohenite is one such metastable phase; free-energy data show that it is unstable with respect to Fe metal + graphite below $T \sim 1070$ K. Its presence in meteorites and metallurgical samples shows that it can form metastably and persist for appreciable periods at lower temperatures.

Free-energy data for haxonite are not available, but the evidence in metal-bearing meteorites offers some information about its stability relative to cohenite. In the IAB iron meteorites, much of the cohenite occupies octahedrally oriented lamellae inside kamacite. This implies that the cohenite precipitated at $T \sim 1100$ K and that the octahedral kamacite nucleated on this cohenite. Haxonite is mainly found in Ni-rich plessite fields and thus nucleated only after appreciable kamacite had grown, thus temperatures were <1000 K. These observations suggest that the Gibbs free energy of the reaction

$$6\ Fe_3C(\text{cohenite}) + 5\ Fe(s) = Fe_{23}C_6(\text{haxonite}) \quad (1)$$

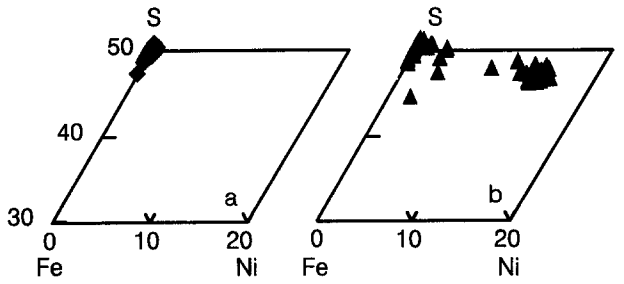

Fig. 10. Compositions of sulfides in carbide-magnetite-bearing L3 (a) and LL3 (b) chondrites.

is close to zero at low temperatures (perhaps 500–1000 K). Haxonite formation may be favored when the activity of Fe is high as it would be in plessite because Fe is ejected from taenite during cooling.

4.1.5. *Nebular formation of carbides and magnetite*

Reaction of nebular CO and H_2 to produce hydrocarbons via the Fischer-Tropsch (FT) synthesis mechanism has been discussed for several decades (e.g., Hayatsu and Anders, 1981) though it appears to be less popular at this time (Cronin et al., 1988). It has also been suggested that FT synthesis in the solar nebula is responsible for the origin of poorly-graphitized aggregates (PGAs) discovered in several OCs (McKinley et al., 1981; Brearley, 1990). PGAs consist of poorly-crytalline graphite, kamacite, pentlandite, troilite, and chromite; carbides and magnetite are absent.

Metallic Fe, the common catalyst in the FT reaction (e.g., Dwyer and Somorji, 1978; Raupp and Delgass, 1979), reacts with the gaseous reactants to produce carbides by a reaction such as

$$3\ Fe(s) + CO(g) + H_2(g) = Fe_3C(s) + H_2O(g) \quad (2)$$

Although the common carbide produced is nonstoichiometric $Fe_{2+X}C$, where X is <0.4 and decreases with time (Pijolat et al., 1987), we use Fe_3C for convenience. At high nebular temperatures in a canonical nebula with $pH_2/pH_2O \sim 1500$ essentially all C is present as CO, but at temperatures below 600 K the equilibrium favors CH_4. However, conversion of CO to CH_4 may be slow enough that CO remains the dominant gas to lower temperatures (Rubin et al., 1988).

Figure 11 shows the calculated equilibrium pCO/pCH_4 ratio and the activity of cohenite (aFe_3C) in nebulae having pH_2 of 10^{-4}, 10^{-5}, and 10^{-6} atm. The curves show that the activity of Fe_3C (aFe_3C) never exceeds 0.01, thus cohenite will not form under equilibrium conditions in the nebula. However, if one assumes that CO fails to convert to CH_4 below 600 K (we used a pCO/pCH_4 of 10), cohenite can reach unit activity at about 500 K, as illustrated by the branch attached to the 10^{-5} atm curve and extending to lower temperatures.

It has been known for decades that at $T < 400$ K in a canonical solar nebula, magnetite is thermodynamically more stable than α- and γ-Fe metal and the other predicted oxidized forms of Fe such as Fe_2SiO_4, etc. There is, however, very little textural evidence for the formation of OC magnetite in the nebula; such magnetite should form a corrosion layer on all metal grains, not the heterogeneously distributed massive grains described in this study.

The lack of nebular stability of cohenite under canonical conditions combined with the observed textural relationships between cohenite, magnetite, and metal make it unlikely that nebular processes were responsible for the formation of carbides.

4.1.6. *Asteroidal formation of carbides and magnetite*

The partial pressures of fluid phases inside a parent body are not easily inferred. The maximum pressure is the overburden pressure, but this will only be achieved if the region is gas tight. Highly unequilibrated chondrites such as LL3.0 Semarkona contain hydrated minerals which formed by reaction with water in an asteroid (Hutchison et al., 1987). Phyllosilicates are also present in EET90161 (this study). There is no information on presence of phyllosilicates in other carbide-magnetite type-3 OCs. It seems likely that formation of phyllosilicates resulted from reactions with water formed during thermal metamorphism by melting of ice that accreted with anhydrous minerals into the LL parent body. At temperatures < 700 K, S_2 pressures are negligible, and the bulk of the gas initially released during metamorphic heating will be H_2O. As temperatures increase above ~400 K, the hydrocarbons will start to break down to CO, CH_4, and other C-bearing gases. Without knowing the amounts and nature of these hydrocarbons, phyllosilicates, and initial ice concentra-

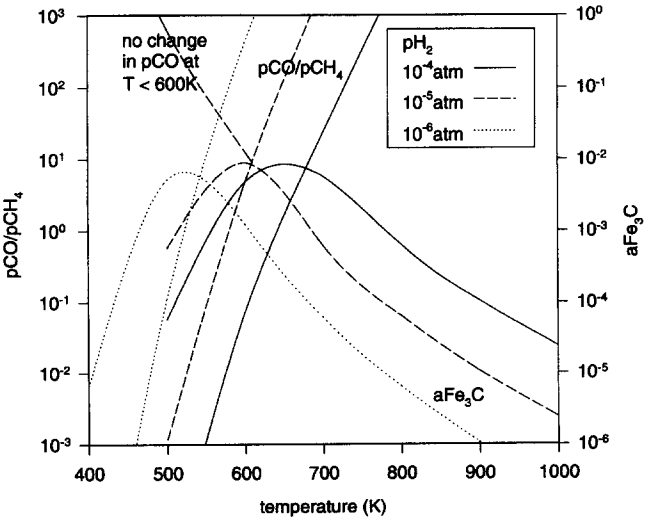

Fig. 11. Equilibrium molar CO/CH_4 ratios in canonical solar nebulae at pH_2 pressures of 10^{-4} atm (solid), 10^{-5} atm (dashed), and 10^{-6} atm (dotted). Under equilibrium conditions Fe_3C does not form a corrosion phase on metallic Fe in canonical nebulae; a maximum activity of $\approx 10^{-2}$ is reached near 600 K. However, if sluggish kinetics prevents CO from converting to CH_4, Fe_3C could form as a metastable phase; the dashed curve extending upwards below 600 K shows the activity if the CO/CH_4 ratio is fixed at 10 at T < 600 K. See text for details.

tions, it is not possible to calculate a pCO/pH_2O ratio in the gas. We suggest that this ratio would have been much less than unity unless and until oxidation reactions used up the bulk of H_2O.

The carbidization reaction 2 of FT FeNi catalysts is probably not important in asteroidal bodies because the partial pressures of H_2 and CO are too low. If we assume a mean pH_2 of 10^{-4} and a pCO of 10^{-2} atm (or, more a propos, that their product is 10^{-6} atm) and $pH_2O = 1$ atm (corresponding to the overburden pressure at a depth of ≈600 m in a chondritic body with a density of 3.5 g cm^{-3} and a radius of 50 km), our calculations show that cohenite could form by reaction 2 at $T < 460$ K.

Additional reactions that can lead to cohenite formation in the asteroidal body are

$$3\ Fe(s) + C(s) = Fe_3C(s) \quad (3)$$

$$3\ Fe(s) + CH_4(g) = Fe_3C(s) + 2\ H_2(g) \quad (4)$$

$$15\ Fe(s) + 4\ CO(g) = 4\ Fe_3C(s) + Fe_3O_4(s) \quad (5)$$

$$3\ Fe(s) + 2\ CO(g) = Fe_3C(s) + CO_2(g) \quad (6)$$

As discussed in the previous section, cohenite is unstable with respect to the elements (Fe and C). Although once formed it can survive metastably, it will not form spontaneously from mixtures of the elements; reaction 3 is thus not important.

Our calculations show that for the reaction 4 to proceed, the pCH_4 needs to be much higher than pH_2. If we assume a pCH_4/pH_2 ratio of 1000 and $pCH_4 = 0.1$ atm, we find that cohenite will only form at $T > 680$ K. Increasing the pCH_4/pH_2 ratio to 10^5 only lowers the minimum stability temperature to 560 K. It is unlikely that this reaction formed cohenite in asteroids, especially in regions that produced low type-3 chondrites, some of which contain hydrated minerals.

Reaction 5 is spontaneous at $T < 700$ K if $pCO > 0.001$ atm, thus it is a possible reaction. Because it permits simultaneous formation of cohenite and magnetite, it may be the strongest candidate for the role of the main reaction involved in the formation of the CMA. As noted above, kinetics may favor the formation of metastable Fe_3C (or haxonite) because of the high activity of atomic Fe resulting from the rejection of Fe from cooling taenite.

Reaction 6 has the interesting consequence that it converts CO(g) to $CO_2(g)$. As discussed earlier, the $pCO_2/pCO < 0.1$ ratio under equilibrium conditions in the presence of Fe metal, but reaction kinetics may allow this reaction to proceed. It offers a possible explanation for the carbonates that are observed in Semarkona (Alexander et al., 1989).

Carbides can be produced by the low-temperature (~200°C) metamorphic tempering of C-bearing martensite, and it is possible that under reducing nebular conditions, C condensed into nebular metal. However, this mechanism is inconsistent with our petrographic observations (e.g., with the common association of carbides with magnetite, zoned textures of some CMA, coexisting carbide, and kamacite inside chondrules) and can be excluded as a major process for the formation of OC CMAs.

We considered three reactions for the formation of magnetite:

$$3\ Fe(s) + 4\ H_2O(g) = Fe_3O_4(s) + 4\ H_2(g) \quad (7)$$

$$Fe_3C(s) + 5\ H_2O(g) = Fe_3O_4(s) + CO(g) + 4\ H_2(g) \quad (8)$$

$$Fe_3C(s) + 4\ H_2O(g) = Fe_3O_4(s) + C(s) + 4\ H_2(g) \quad (9)$$

As noted by Wasson and Krot (1994), in parent bodies a plausible H_2O partial pressure (pH_2O) is 1 atm, equivalent to the overburden pressure at a depth of 1 km in a chondritic asteroid with a density of 3.5 g cm^{-3} and a radius of 50 km. Because H_2 and CO are trapped by adsorption or the products of reaction, it is likely that their partial pressures pH_2 and pCO were significantly less than 1 atm. The first reaction is probably the main reaction if the two reactants are present. Metallic Fe is certainly present in all OC and, as discussed, we infer that $H_2O(g)$ is the most likely oxidant. Equilibrium calculations show that, with $pH_2O = pH_2 = 1$ atm, Fe_3O_4 is stable in metal-bearing asteroids at $T < 1280$ K. If, as expected, $pH_2O > pH_2$, the stability extends to higher temperatures. Reactions 8 and 9 form magnetite by the oxidation of cohenite; the C forms CO(g) and graphite, respectively. If we assume $pH_2O = pCO = pH_2$ in the first case, Fe_3O_4 is stable throughout the range covered by our calculations (300–1400 K). If graphite is formed instead of CO and we assume $pH_2O = pH_2$, magnetite is more stable than cohenite at temperatures < 1250 K. Because of the relatively low Gibbs formation energies of hydrocarbons at the relevant temperatures, C is an adequate substitute for them. These calculations confirm that, as expected, magnetite can form by oxidation of cohenite.

Two of the most carbide-rich, oxidized type-3 OCs, Semarkona (Hutchison et al., 1987; Alexander et al., 1989) and EET90161 (this study) experienced pervasive, though incomplete aqueous alteration to layer-lattice minerals. Olivine, pyroxene, and primary sulfides have been partially replaced by Ca-Na-K-Fe-rich saponite and Fe-Ni sulfides. The products of aqueous alteration may be missing in other CMA-bearing OCs because these products are destroyed even by relatively mild metamorphism.

5. SUMMARY

Based on these arguments and petrographic observations, we suggest that carbide-magnetite-bearing type-3 OCs formed from materials similar to those parental to normal OCs. The CMA-bearing OCs experienced alteration on an asteroid, including carbidization and oxidation. In most cases the carbides and magnetite seem to have formed simultaneously or the carbides formed first. The most probable reaction involves carbidization of Fe-Ni metal by CO gas and simultaneous formation of magnetite. This and similar reactions formed carbides of variable compositions, high-Ni taenite, and Co-rich kamacite. Magnetite was probably also produced by the low-temperature oxidation of Fe-Ni metal and other Fe-bearing phases by H_2O gas that continued after CO gas was depleted and carbidization ceased.

Because this alteration affected only a few H-L-LL3 chondrites, we suggest that their parent asteroids contained rela-

tively small amounts of the necessary fluids and/or that these fluids were heterogeneously distributed or transported. The source of CO gas could have been hydrocarbons from the deep interior oxidized during metamorphism and transported to the surface (Sugiura et al., 1984, 1986). This fluid transport could have proceeded along zones of high fluid permeability that were created during accretion and subsequent impact tectonic events. Carbidization could have been interrupted by the brecciation process as well, and this might explain the coexistence of kamacite-taenite and carbide-magnetite assemblages in brecciated meteorites. Alternatively, brecciation could have been postdated carbidization.

Chondritic parent asteroids accreted complex mixtures of carbonaceous materials, probably of nebular derivation mainly but also including interstellar materials or fragments of other asteroids. All of these components could have contributed to the formation of CO gas that resulted in carbidization of Fe-Ni metal. A detailed study of carbon isotopes in the CMA would help delineate the sources of C.

Acknowledgments—We are grateful to Alan Rubin for discussions and to R. Hutchison and P. Benoit for reviews. We especially thank C. Alexander for his detailed and painstaking comments. We acknowledge C. Manning, D. Winter, and T. Hulsebosh for technical support. Samples were kindly provided by G. J. MacPherson, M. Lindstrom, and by the members of the U.S. Antarctic Meteorite Working Group. This work was mainly supported by NASA grants NAGW-3535 (J. T. Wasson, P. I.), NAGW-3281 (K. Keil, P. I.), and 152-11-40-23 (M. Zolensky, P. I.). This is the Hawaii Institute of Geophysics and Planetology Publication No. 920 and School of Ocean and Earth Science and Technology Publication No. 4162.

Editorial handling: C. Koeberl

REFERENCES

Alexander C. M. O., Barber D. J., and Hutchison R. H. (1989) The microstructure of Semarkona and Bishunpur. *Geochim. Cosmochim. Acta* **53,** 3045–3057.

Anders E. and Grevesse N. (1989) Abundances of the elements: Meteoritic and solar. *Geochim. Cosmochim. Acta* **53,** 197–214.

Bradley J. P., Brownlee D. E., and Fraundorf P. (1984) Carbon components in interplanetary dust: Evidence for formation by heterogeneous catalysis. *Science* **223,** 56–58.

Brearley A. J. (1990) Carbon-rich aggregates in type 3 ordinary chondrites: Characterization, origins, and thermal history. *Geochim. Cosmochim. Acta* **54,** 831–850.

Christofferson R. and Buseck P. R. (1983) Epsilon carbide: a low-temperature component of interplanetary dust particles. *Science* **222,** 1327–1329.

Cronin J. R., Pizzarello S., and Creikshank D. P. (1988) Organic matter in carbonaceous chondrites, planetary satellites, steroids and comets. In *Meteorites and the Early Solar System* (ed. J. F. Kerridge and M. S. Matthews), pp. 819–857. Univ. Arizona Press.

Dwyer D. J. and Somorji G. A. (1978) Hydrogenation of CO and CO_2 over iron foils: correlations of rate, product distribution, and surface composition. *J. Catalysis* **52,** 291–301.

Fraundorf P. (1981) Interplanetary dust in the transmission electron microscope: diverse materials from the early solar system. *Geochim. Cosmochim. Acta* **45,** 915–943.

Fredriksson K., Jarosewich E., and Wlotzka F. (1989) Study Butte: A chaotic chondrite breccia with normal H-group chemistry. *Z. Naturforsch.* **44a,** 945–962.

Goldstein J. I. (1979) Principles of thin-film X-ray microanalysis. In *Introduction to Analytical Electron Microscopy* (ed. J. J. Hren et al.), pp. 813–820. Plenum.

Grossman J. N. (1994) The Meteoritical Bulletin, No. 76, 1994 January: The U.S. Antarctic Meteorite Collection. *Meteoritics* **29,** 100–143.

Hayatsu R. and Anders E. (1981) Organic compounds in meteorites and their origins. *Topics Current Chem.* **99,** 1–37.

Hutchison R., Alexander C. M. O., and Barber D. J. (1987) The Semarkona meteorite; First recorded occurrence of smectite in an ordinary chondrite, and its implication. *Geochim. Cosmochim. Acta* **51,** 1875–1882.

JANAF (1985) *JANAF Thermochemical Tables,* 3rd ed. Amer. Chem. Soc.

McKinley S. G., Scott E. R. D., Taylor G. J., and Keil K. (1981) A unique type 3 ordinary chondrite containing graphite-magnetite aggregates—Allan Hills A77011. *Proc. Lunar Planet. Sci. Conf.* **12,** 1039–1048.

McSween H. Y. and Labotka T. C. (1993) Oxidation during metamorphism of the ordinary chondrites. *Geochim. Cosmochim. Acta* **57,** 1105–1114.

Mendybaev R. A., Kuyunko N. S., Lavrukhina A. K., and Khodakovsky I. L. (1989) Kinetic analysis of stability of interstellar carbon in preplanetary nebula. *Geokhim.* **49,** 467–477.

Ohsumi K., Miyamoto M., Takase T., Kojima H., and Yanai K. (1994) Diffraction profile analysis olivines in thin sections of meteorites by the miro-region Laue method using synchrotron radiation. *Proc. NIPR Symp. Antarctic Meteor.* **7,** 244–251.

Perron C., Bourot-Denice M., Pellas P., and Marti K. (1990) Si-, P-, Cr-bearing inclusions in Fe-Ni of ordinary chondrites. *Meteoritics* **25,** 398 (abstr.).

Pijolat M., Perrichon V., and Bussiere P. (1987) Study of the carbidization of an iron catalyst during the Fischer-Tropsch synthesis: Influence on its catalytic activity. *J. Catalysis* **107,** 82–91.

Raupp G. B. and Delgass W. N. (1979) Mössbauer investigation of supported Fe and FeNi catalysts. II. Carbides formed by Fischer-Tropsch synthesis. *J. Catalysis* **58,** 348–360.

Robie R. A., Hemingway B. S., and Fisher J. R. (1978) Thermodynamic Properties of Minerals and Related Substances at 298.15 K and 1 Bar (10^5) Pascals) Pressure and at Higher Temperatures. *USGS Bull.* **1452.**

Rubin A. E. (1990) Kamacite and olivine in ordinary chondrites: Intergroup and intragroup relationships. *Geochim. Cosmochim. Acta* **54,** 1217–1232.

Rubin A. E., Fegley B., and Brett R. (1988) Oxidation state in chondrites. In *Meteorites and the Early Solar System* (ed. J. F. Kerridge and M. S. Matthews), pp. 488–511. Univ. Arizona Press.

Scorzelli R. B., Petrick S., and Krot A. N. (1996) Iron-57 Mössbauer studies of carbide-magnetite-bearing type 3 ordinary chondrites. *Meteoritics Planet. Sci.* **31,** A125.

Scott E. R. D. (1971) New carbide, $(Fe, Ni)_{23}C_6$, found in iron meteorites. *Nature Phys. Sci.* **229,** 61–62.

Scott E. R. D. (1984) Pairing of meteorites found in Victoria Land, Antarctica. *Mem. NIPR Spec. Issue* **35,** 102–125.

Scott E. R. D., Taylor G. J., and Maggiore P. (1982) A new LL3 chondrite, Allan Hills A79003, and observations on matrices in ordinary chondrites. *Meteoritics* **17,** 65–75.

Sears D. W. G., Hasan E. A., Batchelor J. D., and Lu J. (1991) Chemical and physical studies of type 3 chondrites—XI: Metamorphism, pairing, and brecciation of ordinary chondrites. *Proc. Lunar Planet. Sci. Conf.* **21,** 495–512.

Sugiura N., Brar N. S., Strangway D. W., and Matsui T. (1984) Degassing of meteorite parent bodies. *Proc. Lunar Planet. Sci. Conf.* **14,** B641–B644.

Sugiura N., Arkani-Hamed J., and Strangway D. W. (1986) Possible transport of volatile trace elements in meteorite parent bodies. *Mem. NIPR Spec. Issue* **46,** 216–225.

Taylor G. J., Okada A., Scott E. R. D., Rubin A. E., Huss G. R., and Keil K. (1981) The occurrence and implications of carbide-magnetite assemblages in unequilibrated ordinary chondrites. *Lunar Planet. Sci.* **12,** 1076–1078 (abstr.).

Wasson J. T. and Krot A. N. (1994) Fayalite-silica association in unequilibrated ordinary chondrites—evidence for aqueous alteration on a parent body. *Earth Planet. Sci. Lett.* **122,** 403–416.

Zolensky M. E. and Thomas K. T. (1995) Iron and iron-nickel sulfides in chondritic interplanetary dust particles. *Lunar Planet. Sci.* **26,** 1567–1568 (abstr.).

APPENDIX A

Pairing and Classification

Pairing of carbide-magnetite-bearing type-3 ordinary chondrites from Lewis Cliff and Elephant Moraine

Pairing of type-3 OC from Antarctica is a complicated problem for several reasons: unknown coordinates resulting from subsequent transport by ice and wind, unknown or poorly constrained terrestrial ages of the meteorites, terrestrial alteration, limited number of analytical data, etc. Scott (1984) paired many L3 chondrites with ALHA77011 (L3.5) based mainly on the presence and abundance of poorly-graphitized aggregates (PGAs) which consist of poorly-crystallized graphite, kamacite, pentlandite, troilite, and chromite (Brearley, 1990). Although the origin of these aggregates is unclear (e.g., Brearley, 1990; Mendybaev et al., 1989) and some of them were possibly added during regolith formation, their unusual but simple mineralogy and rarity make them very useful for pairing studies. The presence and texture of CMAs offer similar clues.

The following criteria were used for pairing: (1) mineralogy and textures of CMAs, (2) chemical compositions of carbides and metal, (3) relative abundances of CMAs and metal-troilite nodules, (4) textures of the host meteorites, their shock stages, and weathering categories, (5) ice-field locality. These data and the results of the pairing are summarized in Table 2.

Two sets of meteorites from Lewis Cliff (Table 2) appear to represent independent falls. The first set consists of two pairs of meteorites: LEW86102 and LEW86105 and LEW85434 and LEW85437, each of which have been previously paired and classified as H3 and L3, respectively. Although these meteorites were found on different ice-fields (Lower Ice Tongue and Upper Ice Tongue), they have nearly identical petrographic and mineralogic properties (Table 2). The second set consists of previously unpaired chondrites including LEW87208, LEW87248, LEW87254, and LEW87284. All were found on the same ice-field (Upper Walcott Neve) and have similar textures, shock stages, weathering categories, and mineralogy of CMAs. The differences in chemistry of carbides and Fe-Ni metal are minor (Figs. 6d–o, 7). Cohenite was not found in LEW87208 and LEW87284, but it is also rare in LEW87248 and LEW87254. Although Co-rich kamacite was not observed in LEW87248, it occurs as small grains coexisting with low-Co kamacite in the other meteorites and could have been missed because of the limited number of microprobe analyses. Thermoluminescence (TL) data published only for LEW87248 and LEW87254 (Sears et al., 1991) show similar TL sensitivity (0.05 ± 0.02 and 0.05 ± 0.01), but different TL peak temperatures (145 ± 6 and 118 ± 3) and peak widths (150 ± 4 and 89 ± 6, respectively). However, because large variations in TL parameters are known for other paired samples (ALHA77011 and ALHA77167 meteorites; Sears et al., 1991), the TL data are not inconsistent with proposed pairing.

Three sets of meteorites among six carbide-magnetite-bearing chondrites from Elephant Moraine may represent one to three independent falls; all six were found on the Texas Bowl Ice-field (Table 2). The first set consists of EET87735, EET90161, EET90261, and EET90519. Cohenite and haxonite are both abundant in these meteorites; magnetite is minor and metal-troilite particles are absent. The chondrites EET90628 and EET90083 may be independent falls. Magnetite and haxonite are both abundant in EET90628; the latter has higher Co contents than haxonite in EET87735 and relatives; cohenite and metal-troilite particles were not observed. Only a few CMAs were found in the small thin section of EET90083 available for study, frustrating attempts at comparison with CMAs in other meteorites from Elephant Moraine. However, EET90083 is the only carbide-magnetite meteorite from this location which has abundant metal-troilite particles and fragments of CMAs, possibly indicating brecciation. The coexistence of CMAs and metal-troilite nodules in brecciated chondrites (e.g., Ngawi and ALHA77278) supports this suggestion. Although tentatively we conclude that these six carbide-magnetite chondrites from Elephant Moraine represent three independent falls, we cannot exclude that the observed differences reflect the actual magnitude of mineralogical variations in large meteorites.

Classification of carbide-magnetite-bearing type-3 ordinary chondrites

Carbide-magnetite assemblages were found among H3, L3, and LL3 chondrites. The majority of the Antarctic carbide-magnetite L3 and LL3 chondrites are of low apparent petrographic subtypes, although they have been classified in only a preliminary manner based on the compositional variations of mafic silicates and metal abundances (Table 2). Because carbides are the dominant opaque phases in many of these chondrites and their optical properties are roughly similar to those of taenite and kamacite, it seems likely that carbide grains were counted as metal during the preliminary classifications and the metal abundances were, therefore, considerably overestimated. In addition, although the Co content in kamacite is a useful parameter in the classification of L3 and LL3 chondrites (Rubin, 1990), large and overlapping ranges in the Co contents of kamacite from carbide-magnetite L3 and LL3 chondrites (and other L and LL chondrites with type number <3.4) make this classification of limited use. Accordingly, additional information is required to properly classify these meteorites into L and LL groups.

In contrast, the H3.8 RKPA80206 and H3.7 WIS91627 are probably well-classified based on chemistry of mafic silicates (Grossman, 1994) and kamacite (this study) as H3. Because the three H chondrites have only a few CMAs, the possibility that they are polymict breccias containing fragments of carbide-magnetite-bearing L3 or LL3 chondrites must be explored. Study Butte is a complex H3-6 regolith breccia (Fredriksson et al., 1989). Although kamacite grains in carbide-magnetite-bearing H chondrites show large ranges in Co content (Fig. 2c, f, i) which are outside the typical range observed in H chondrites (Rubin, 1990), as discussed above, these are disequilibrium assemblages. Because there appear to be resolvable differences in mineralogy and chemistry of CMA in H, L, and LL chondrites, and no L or LL silicate material have been found in Study Butte (Fredriksson et al., 1989), we conclude that the CMAs are not confined to foreign clasts. Carbides in H chondrites are intimately associated with large kamacite grains which have relatively low Co concentrations, and kamacite grains in CMAs in L and LL chondrites are rare and typically Co-rich (Figs. 2, 4, 6, 9). Carbides in H chondrites have much lower mean Co contents than those in L and LL chondrites, which are possibly inherited from the compositional differences of metal replaced by CMA.